 doi:10.20944/preprints202012.0232.v1

Review

Liquid-Based Reconfigurable Antenna Technology: Recent Developments, Challenges and Future

Habshah Abu Bakar [1], Rosemizi Abd. Rahim [2,*], Ping Jack Soh[3], and Prayoot Akkaraekthalin[4,*]

[1] Department of Electrical Engineering, Politeknik Sultan Abdul Halim Muadzam Shah, Jitra 06000, Kedah, Malaysia; abubakarhabshah@gmail.com
[2] Faculty of Electronic Engineering Technology, Universiti Malaysia Perlis, Pauh Putra Campus, Pauh 02600, Perlis, Malaysia
[3] Advanced Communication Engineering (ACE) Centre of Excellence, Faculty of Electronic Engineering Technology, Universiti Malaysia Perlis, Kangar 01000, Perlis, Malaysia; pjsoh@unimap.edu.my
[4] Department of Electrical and Computer Engineering, Faculty of Engineering, King Mongkut's University of Technology North Bangkok (KMUTNB), 1518 Pracharat 1 Rd., Wongsawang, Bangsue, Bangkok 10800, Thailand
* Correspondence: rosemizi@unimap.edu.my (R.A.R.); prayoot.a@eng.kmutnb.ac.th (P.A.)

Abstract: Advances in reconfigurable liquid-based reconfigurable antennas are enabling new possibilities to fulfil the requirements of more advanced wireless communication systems. In this review, a comparative analysis of various state-of-the-art concepts and techniques for designing reconfigurable antennas using liquid is presented. First, the electrical properties of different liquids at room temperature commonly used in reconfigurable antennas are identified. This is followed by a discussion of various liquid actuation techniques in enabling high frequency reconfigurability. Next, liquid-based reconfigurable antennas in literature used to achieve the different types of reconfiguration will be critically reviewed. These include frequency-, polarization-, radiation pattern- and compound reconfigurability. The current concepts of liquid-based reconfigurable antennas can be classified broadly into three basic approaches: altering the physical (and electrical) dimensions of antennas using liquid, applying liquid-based sections as reactive loads; and implementation of liquids as dielectric resonators. Each concept and their design approaches will be examined, outlining their benefits, limitations, and possible future improvements.

Keywords: reconfigurable antennas; liquid antennas; liquid actuation techniques

1. Introduction

Antennas is one of the critical parts in wireless communication system which must be designed and deployed efficiently so that it could effectively accommodate multiple wireless services at the same time [1]. Traditionally, conventional antennas are designed for a fixed frequency band, radiation pattern and polarization. However, with the rapid development of wireless communication standards, reconfigurable antennas are needed to support possible changes in system requirements or environmental conditions.

Reconfigurable antennas offers the capability to change to different antenna characteristics to adapt the dynamic wireless communication systems [2]. Reconfigurability is defined as the ability of antenna to change its operational frequency, radiation pattern, polarization and other properties by using different techniques. Conventional reconfigurable antennas typically employ Radio Frequency (RF) switches such as Microelectromechanical systems (MEMS), PIN diode [1, 3] and varactors [4–6]. MEMS offers high isolation and low insertion loss [7], whereas PIN and varactor diodes are popular for fast switching and low power consumption [8].

 doi:10.20944/preprints202012.0232.v1

Although the feature of reconfigurability can be achieved using RF switches, antennas can also be integrated with conductive fluids such as liquid metal and ionized water and dielectric fluid such as ethyl acetate and de-ionized (DI) water to cater to tunability, and to be combined with flexibility and other sensing functionalities in wireless communication. Moreover, the recent introduction of liquid metals such as Galinstan and EGaIn with excellent electrical and thermal conductivity, non-toxicity and the unique physical properties adds on to the prospect of implementing such reconfigurable antenna designs. Liquid-metal have utilized applied pressure actuation using syringe or micro pump [9,10] or electrical actuation like electrocapillary actuation (ECA), continuous electrowetting (CEW), and electrochemically controlled capillary (ECC) [11]. Recent implementations of liquid metal in reconfigurable antennas include the likes of monopoles [12,13], dipoles [14], helical [15] planar inverted-Fs [16] , slot antennas [17,18] and Yagi-Uda antennas [9].

Non-toxic liquid metal has been implemented for frequency reconfigurability [19–21], polarization reconfigurability [22,23], radiation pattern reconfigurability [24], gain reconfigurability [25] and the combined reconfiguration of multiple parameters, or compound reconfigurability [14]. Past available reviews discussing the different aspects liquid-based antennas are as follows. First, the research progress on the fabrication techniques for microfluidic electronics, specifically focused on stretchable substrates, their issues and future challenges was reported in [8]. Besides that, [11] reviewed the manipulation of interfacial tension of liquid metals using voltage for antenna reconfiguration. The major challenges in the fabrication processes of gallium-based liquid metal is discussed in [26], whereas the review in [27] focused on the unique properties and applications of gallium-based alloys. The development of antennas using conductive and dielectric liquids has been presented in [28]. Meanwhile, the use of different substrates and conductive fluids, including their fabrication techniques to achieve single antenna reconfigurability was reviewed in [29]. Finally, the design techniques, advantages and limitations of liquid-based antennas, specifically focused on dielectric liquids are reviewed in [30]. Despite these literatures, none of these reviews have focused on the detailed concepts, design approaches and implementation of conductive and dielectric liquids into different types of reconfigurable antennas, which include single parameter and compound reconfiguration.

This paper reviews recent progress on reconfigurability of antenna using conductive and dielectric fluids, including their concepts, designs and implementations. This article covers four underlying areas of focus. First, it is focused primarily on non-toxic gallium-based alloys, which exists in liquid form when being close to or at room temperature. Besides that, its properties and available liquid metal actuation techniques are presented in Section II. The next focus of this work is on analyzing techniques which have been utilized to achieve various types of antenna reconfigurability using liquids in Section III and IV. Finally, a future perspective of such mechanism, highlighting the life expectancy of these liquids concludes this article.

2. Non-Toxic Liquid Metals

There are five metals are capable to remain as liquid metals at room due to their low or close-to-room-temperature melting points. They include caesium (Cs), francium (Fr), gallium (Ga), mercury (Hg) and rubidium (Rb) [27]. The explosive reaction of Cs and Rb, radioactivity of Fr and toxicity of Hg limit their practical applications to specialized areas [31]. Gallium, on the other hand, can be combined with other metals to create the binary alloy, eutectic gallium indium (EGaIn) and ternary alloy gallium, indium, and stannum (Galinstan), also known as non-toxic liquid metals. The use of such non-toxic, Gallium-based alloys is growing steadily in reconfigurable antenna technology [32].

Preprints (www.preprints.org) | NOT PEER-REVIEWED | Posted: 9 December 2020 doi:10.20944/preprints202012.0232.v1

Liquid metals near or below room temperature offer great potential in the development of innovative antenna technology for realizing stretchable antennas [33], flexible antennas [34] and reconfigurable antennas [21, 34]. This is due to their capability in maintaining stable electrical functions despite the shape deformation caused by stretching and compression. Besides that, Gallium-based liquid metals also features low toxicity, unique chemical properties and excellent electrical conductivity [36]. Galinstan and EGaIn are two of the Gallium-based alloys which exist in room temperature. Manipulation of their physical and chemical properties can potentially contribute to the development of flexible and reconfigurable antennas.

2.1 Properties of Non-Toxic Liquid Metal

Galinstan is a Geratherm Medical AG licensed trademarks in Germany. It is an odourless and silvery liquid which exists at room temperature, composed of metal components gallium (68.5%), indium (21.5%) and tin or stannum (10%). It features an excellent electrical and thermal conductivity and unique chemical properties. It has low melting point of -19°C, a boiling point of above 1300 °C and thermal conductivity of 16.5 W/mK. Due to the uniqueness of its chemical properties and its low-toxicity, Galinstan is an ideal alternative for mercury, which was previously employed in miniaturized devices. [37].

On the other hand, EGaIn is an electrically conductive liquid metal composed of 75.5% Gallium and 24.5% indium. Its physical properties are similar with Galinstan, as summarized in Table 1, featuring a higher melting point and boiling point compared to Galinstan, at about 15.5°C and 2000°C.

Table 1. Summary of the properties of Galinstan and EGaIn, adapted from [8,36].

Properties	Galinstan	EGaIn
Material composition	Gallium (68.5%), indium (21.5%) and tin or stannum (10%).	Gallium (75.5%) and indium (24.5%)
Appearance at room temperature	Liquid	Liquid
Color	Silver	Silver
Melting point(°C)	-19	15.5
Boiling Point (°C)	>1300	2000
Viscosity (Pa.s)	2.4×10^{-3}	2.0×10^{-3}
Density (kg/m^3)	6440	6280
Surface tension (N/m)	0.718	0.624
Electrical conductivity (S/m)	3.46×10^6	3.4×10^6
Thermal conductivity (W/m.K)	16.5	26.4

2.2 Liquid Metal Actuation in Reconfigurable Antenna

Conventionally, liquid metal can be actuated using manual pneumatic actuation, either in the form of syringe as its simplest form [37,38], or by pneumatic actuation via the application of pressure using air bubble [40] using a pump or micropump [41]. Besides that, electronic actuation techniques such as ECA, CEW and ECC using voltage difference are effective to control the interfacial or surface

Preprints (www.preprints.org) | NOT PEER-REVIEWED | Posted: 9 December 2020 doi:10.20944/preprints202012.0232.v1

tension of liquid metal. The basic mechanism of ECA is enabled by changing the surface tension of liquid metals using electrical potential charges at the boundary between two fluids, i.e. liquid metal and electrolyte. In other words, the charges in the electrical bias are used to change the surface tension, thus deforming the shape of liquid metal in response to voltage. On the other hand, CEW operates based on variation in the gradients of the surface tension of the liquid metal [11]. The continuous change in the liquid metal surface wetting properties is caused by the potential drop of the liquid metal in an electrolyte caused by electrocapillary, thereby allowing the liquid metal to be actuated within the channel. The third method, which is the ECC method works based on the decrease of interfacial tension of the liquid metal by adding strong acids or bases. This is to continuously remove or reduce the excessive oxide layer that prevents direct contact between the liquid metal and its surroundings. In comparison to CEW, changes in ECC in moving the liquid metal in the reservoir towards the capillary is more significant in response to the bias voltage, as illustrated in Figure 2 [21]. Figure 1 illustrates the comparison between ECA and CEW.

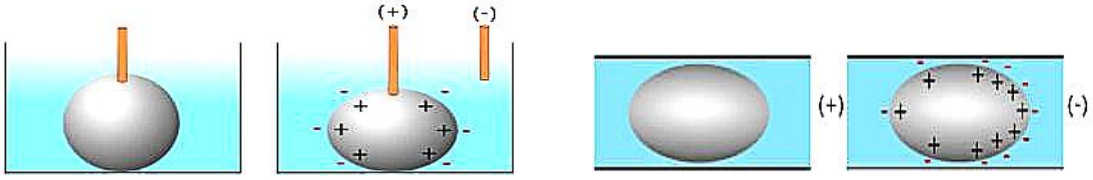

Figure 1. Illustrative comparison between (a) ECA and (b) CEW [11].

Figure 2. Illustration of the mechanism of (a) CEW and (b) ECC [21].

In [42], two flexible tubing have been inserted into holes to serve as liquid metal inlet and outlet for the antenna structure. A manual liquid actuation has been implemented by inserting syringes to inject the liquid into microchannel. This antenna has showed the same performance despite its channel being repeatedly washed using Teflon and refilled with Galinstan. The fluid inlet and outlet also has been introduced in [40], where a syringe is used to generate the pressure-driven air bubble actuation. In [32], the applied air pressure using syringe is used to control the physical length of the antenna. This process, while remaining repeatable and reversible, results in less radio frequency losses than CEW actuation. However, such manual actuation method is limited in terms of switching speed.

The automatic actuation of liquid metal using a computer-controlled syringe pump has been proposed and implemented in [16]. This pump can infuse and withdraw liquid metal in the upper arm of planar inverted-F antenna, allowing it to control its electrical length. A vector network analyser (VNA) and syringe pump are connected to the control computer, resulting in a bulky system. Conversely, such system can be more practical and compact if a micropump is used in their place. The use of such micropump has been demonstrated in [10], where the amount of liquid metal injected

Preprints (www.preprints.org) | NOT PEER-REVIEWED | Posted: 9 December 2020 doi:10.20944/preprints202012.0232.v1

into the microfluidic channels is determined using a micropump activated using a microcontroller. It has been also demonstrated in [42,12] that the physical length of the antenna can be reconfigured using bidirectional micropump units. This is done by retracting a portion of the volume of liquid-metal to reside over the feed line of the microstrip. Besides that, this reconfiguration technique also depends on the ability of the antenna to form a continuous liquid-metal slug in microfluidic channel. A peristaltic pump has been used to actuate the Galinstan flow for the helical antenna in [44]. Using a Raspberry Pi computer, the peristaltic pump is controlled via an H-bridge circuit that can continually adjust the pump speed and direction. For applications requiring compact sizes, the size of the micropump unit might be of concern in practice.

In [45], liquid metal was actuated electrically using ECA to place the liquid metal in polyimide channels. The applied DC voltage will manipulate liquid metal surface tension, causing motion towards positive bias. However, the DC bias must be supplied continuously to avoid the liquid metal withdrawing back to its original position. To overcome this need, a metastable locking method that extends the ECA concept is employed. Metastable locking can be achieved by implementing notches in the fluidic channel. The liquid metal extends to fill a notch in the channel, producing a minimal localized surface energy and rests the liquid metal in the notch. A DC bias with reverse polarity is supplied for the purpose of releasing the liquid metal from that notch. The same method has also been implemented in [46].

The antenna presented in [47] implemented the CEW to induce motion of liquid metal based on its surface tension. When liquid metal is immersed in an electrolyte, the exchange of ions results in a net charge acquisition on the surface of the fluidic metal (Figure 3). This surface charge draws opposite charged ions from the adjacent electrolyte onto the polarizable interface, forming an electrical double layer (EDL). The motion of the liquid metal occurs due its attempt to minimize its surface energy by "wetting" it to the lower surface tension.

(a) (b)

Figure 3. (a) Liquid metal in an electrolyte. (b) Potential gradient across the electrolyte [47].

The CEW method also has been used in [25]. The gain of the reconfigurable antenna is controlled by applying a voltage bias through an electrolyte to induce the slug of Galinstan along the channel. This then tunes the length of stub and antenna gain. In [48], the CEW method is used to switch on and off the pixelated dipole by actuating the liquid metal to the top and bottom of the antenna reservoir. This technique controls the liquid metal tuning automatically, besides reducing the microscale device dimensions. Such concept paves the way for future submillimeter-dimensioned systems.

A monopole antenna presented in [21] implemented the ECC method by supplying a DC potential between the EGaIn reservoir and electrolyte. The positive supply to the liquid metal increases the oxidation of the leading surface and reduces the surface tension of the metal fluid. This then moves the liquid metal towards the electrolyte in the capillary. Changing the voltage polarity will withdraw the liquid metal back into the reservoir, which also changes the shape and position of the antenna. On the other hand, ECC has been used in the cylindrical helical antenna to alter the

Preprints (www.preprints.org) | NOT PEER-REVIEWED | Posted: 9 December 2020 doi:10.20944/preprints202012.0232.v1

length of liquid metal in the microfluidic channel in [49]. The EGaIn oxide layer which has been produced electrochemically increases the interfacial tension of liquid metal, thus driving the liquid metal to the channel. Such concept has also been applied in [14], where four independent DC bias voltages are applied to two pairs of dipole arms containing EGaIn liquid metal and electrolyte to control the lengths of each individual arm. The ECC method allows simultaneous injection or withdrawal of liquid metal from multiple capillaries. In addition to that, the use of strong acid and bases in the ECC method helps to continually remove excessive oxidation layers. In the following sections, examples of reconfigurable antennas using non-toxic liquid metal based on different design concepts and applied technology will be discussed.

3. Design Concepts of Non-Toxic Liquid Metal Reconfigurable Antennas

The interest in reconfigurable antennas in the past few years has grown due to their capability of enabling tunability and switchability in antenna designs. While the implementation of RF switches such as PIN diodes [1,3,18,48,49] have increased the growth of such versatile antennas, the number and range of switching states increases with the increase of circuit complexity [21]. This motivated the choice of metal fluids, which changes the antenna characteristics using fluid flow as an alternative for antenna reconfiguration. In recent years, various unique and novel concepts of reconfigurable antennas using liquid metals have been developed. Several key aspects of antenna reconfiguration will be addressed in the following sections, with examples of antenna structures for different types of reconfigured parameters. The three main types of reconfigurable parameters are frequency reconfiguration, polarization reconfiguration and other reconfigurations (compound, gain, phase shifting and directivity reconfiguration).

3.1. Frequency Reconfigurable Antennas

Frequency reconfigurable antenna has become an important feature in modern communication systems. There are commonly two design approaches for achieving frequency reconfigurability, which are by altering the physical size of antenna and reactive loading of liquid metal. Other possible techniques to achieve frequency reconfigurability will also be explained.

3.1.1. Physical/ Electrical Size Modification

Manipulating the length of the microstrip feed line and radiating aperture of a slot antenna to enable the frequency tuning has been studied in [40], as shown in Figure 4.

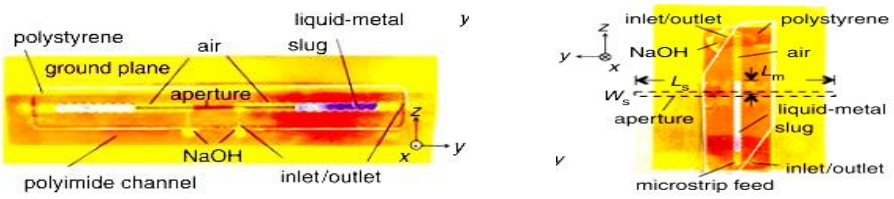

(a) (b)

Figure 4. Fluidic slot antenna. (a) Liquid metal slugs in aperture. (b) Liquid metal slug in microstrip line [40].

Two fluidic channels are fabricated at either ends of the aperture and microstrip feed line. Air pressure difference is created between the two sides of the Galinstan slugs by pneumatically pumping the liquid using a syringe. Air bubble will drive the slugs within the fluidic channels to adjust the length of the feed line and radiating aperture, thus achieving frequency reconfigurability.

Preprints (www.preprints.org) | NOT PEER-REVIEWED | Posted: 9 December 2020 doi:10.20944/preprints202012.0232.v1

This slot antenna achieved a 26 % tunable bandwidth, ranging from 1.42 to 1.84 GHz. This method, while remaining repeatable and reversible, results in less radio frequency losses than CEW actuation. The disadvantage of this method is the longer actuation time (of about 1s) due to the use of syringe for pneumatic actuation.

Next, a frequency reconfigurable antenna using electrically actuated Galinstan is proposed in [47]. Frequency agility is enabled using a Galinstan slug by varying the slot aperture, thus changing the resonant frequency of antenna. An interlocking circular channel made using PDMS is fabricated at two ends of the aperture and overlaps the slot line on each side. Polyimide tape is used to bond the PDMS fixture to the ground plane and to separate the liquid metal from copper, as illustrated in Figure 5. A 8Vpp, +3VDC square wave signal is applied to actuate the liquid metal towards the lower surface tension. The proposed antenna increased the operational frequency from 2.78 to 3.63 GHz and achieved the 36 % of total effective tuning bandwidth.

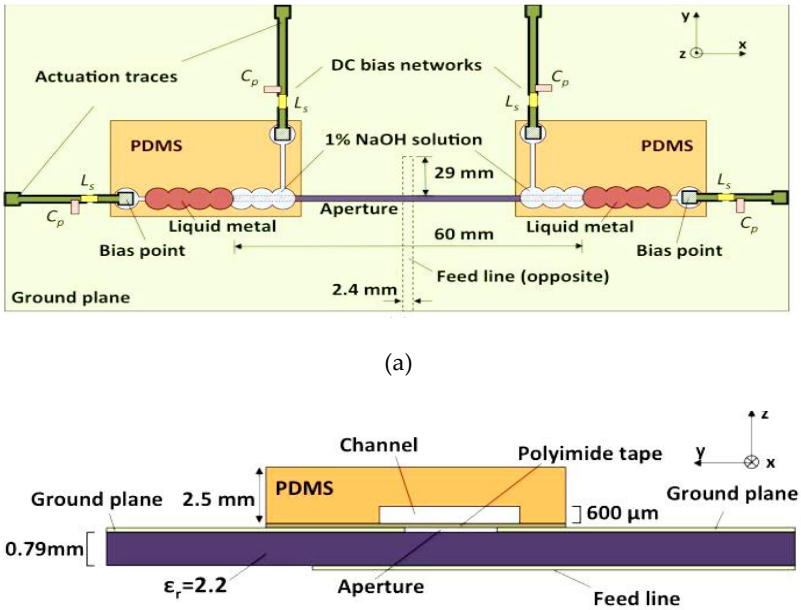

(a)

(b)

Figure 5. Frequency reconfigurable antenna. (a) Top view. (b) Side view [47].

Meanwhile, the upper arm of a planar inverted-F antenna (PIFA) integrated with Galinstan liquid metal was presented in [16]. The Galinstan liquid is filled in a Teflon tube, as shown in Figure 6.

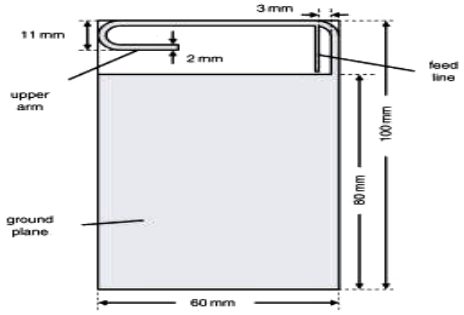

Figure 6. Planar inverted-F antenna (PIFA) [16].

Experiments validated that the changes in the length of the Galinstan-filled portion changes the operating frequency. This antenna is capable of automatically tuning back to the 720 MHz resonant

Preprints (www.preprints.org) | NOT PEER-REVIEWED | Posted: 9 December 2020 doi:10.20944/preprints202012.0232.v1

frequency after an interference from the human hands placed near the antenna. However, the use of the syringe pump in this design is not practical for antenna application.

Another example of frequency reconfigurable antenna with 3D printed microfluidic channel and composite tuning slots is presented in [41]. Two slots are inserted on a patch and the microfluidic channel is bounded on top of the slotted patch, as shown in Figure 7. By loading the liquid metal into the microfluidic channel, the length of liquid metal is altered, and thus produced 70 % of frequency tuning bandwidth from ranged from 2 to 3.5 GHz.

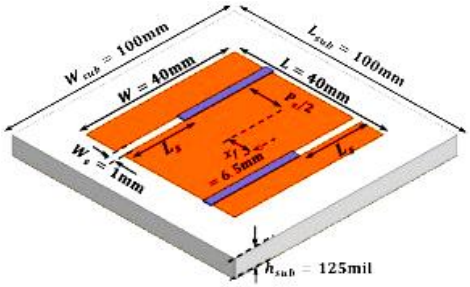

Figure 7. Patch antenna with two slotted patch [41].

In [32], the frequency tunability of a fluidic antenna is enabled by changing the liquid metal feedline. In this design, a bottom and top plate are bonded together to form fluidic channels using plasma treatment. The feedline is designed in a "7"-shaped digital number, whereas a square-shaped patch with "6"-shaped pattern fluidic channel was fabricated on PDMS and filled with Galinstan, as seen in Figure 8. Air pressure is applied to control the physical length of the fluidic slug. The inlet and outlet ports are connected to the feedline and all fluidic channels to enable fluid injection. It has been demonstrated that by manipulating the length of the fluidic slug, the frequency range can be tuned from 2.2 GHz to 9.3 GHz.

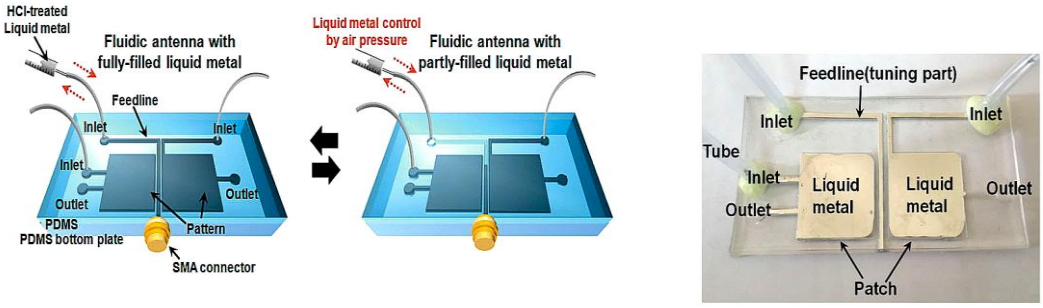

(a) (b)

Figure 8. The proposed frequency tunable antenna. (a) Schematic antenna. (b) Fabricated antenna [32].

Next, a tunable dual-band patch antenna has been studied in [52]. This antenna was implemented using the 3D printing technique on a Polymethylmethacrylate (PMMA) substrate, and channels on a double patch antenna was fabricated using Fused Deposition Modeling (FDM). The PMMA channel consists of three layers, namely the foundation layer, the liquid metal channel, and the cover layer. A liquid metal channel with a width of 2.2 mm is used to connect (ON configuration) or disconnect (OFF configuration) the two patches, as shown in Figure 9. The external voltage is supplied to re-drain and refill the liquid metal into the channels to achieve frequency reconfigurability. The two side channels are introduced to separate the boundaries of Galinstan and NaOH. This design includes a biasing circuit using a quarter wavelength inductive line and a DC

Preprints (www.preprints.org) | NOT PEER-REVIEWED | Posted: 9 December 2020 doi:10.20944/preprints202012.0232.v1

blocking capacitor. The use of the capacitor lead to self-resonance, while the implementation of the 90° radial stub was aimed to obtain a wideband frequency. The simulated centre frequency for the OFF and ON configurations ranges from 14.2 GHz (with a bandwidth of 0.66 GHz) to 15.1 GHz (with a bandwidth of 0.88 GHz), respectively.

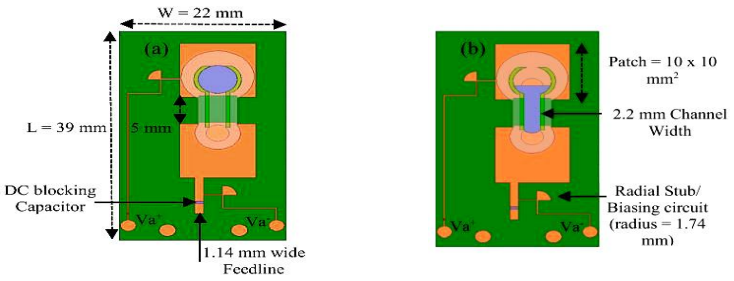

(a) (b)

Figure 9. Dual patch antenna. (a) OFF configuration. (b) ON configuration [52].

In another study presented in [53], a frequency-reconfigurable wearable antenna is proposed. This loop antenna was prototyped by injecting the Galinstan liquid metal into silicon tubing, as shown in Figure 10. Two conductive pins with silicon-based glue was inserted into the tubing ends to avoid the leakage of the liquid metal. This design operated at 868 MHz and can be tuned to 2.45 GHz. Advantages of this approach includes simplicity in prototyping, high flexibility, stretchability and ease of integration into wearable devices.

(a) (b)

Figure 10. The proposed wearable antenna. (a) Galinstan and silicon tubing. (b) Loop antenna [53].

3.1.2. Reactive Loading of Liquid Metal

An example of the reactive loading technique involves the integration of Galinstan liquid metal into slot structures to achieve frequency reconfigurability in a coplanar waveguide (CPW)-fed folded slot antenna in [17]. In this design, two pairs of Galinstan-filled microchannels are used to achieve the frequency tuning of three operating frequencies, 2.4, 3.5, and 5.8 GHz, as depicted in Figure 11. The two pairs of microfluidic channels are separated using two separate polydimethylsiloxane (PDMS) structures. The reactive loading effect is enabled by placing Galinstan bridges on top of the folded slot to tune the antenna frequency, offering size miniaturization and a very wide switching range from 2.4 to 5.8 GHz with

Preprints (www.preprints.org) | NOT PEER-REVIEWED | Posted: 9 December 2020 doi:10.20944/preprints202012.0232.v1

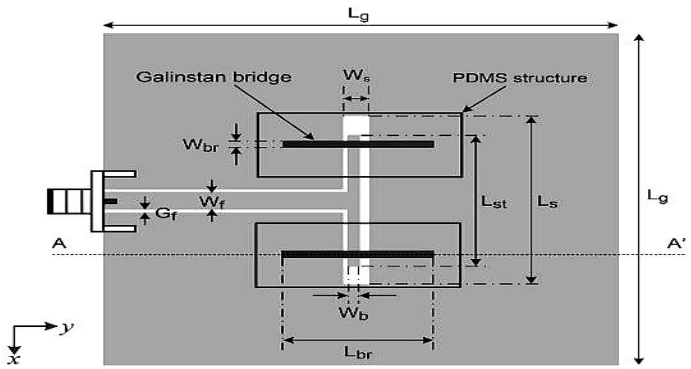

Figure 11. The CPW folded slot antenna with Galinstan bridges **[17].**

The switchable dual band slot antenna proposed in [42] achieves an overall frequency coverage ratio of 3:1 (1.8 to 5.4 GHz). In this design, five microchannels for Galinstan liquid metal are separated by two spin coated PDMS structures. By filling or emptying the Galinstan bridges illustrated in Figure 12, the antenna can be switched to operate in a dual band mode. The Galinstan bridges provide the reactive loading effect which can be used to independently control the operating frequency of the antenna. The proposed design provides a frequency tuning range of 1.8 to 3.1 GHz (in the first band) and 3.2 to 5.4 GHz (in the second band). A high radiation efficiency of about 78 % and 82 % is featured in each band, respectively.

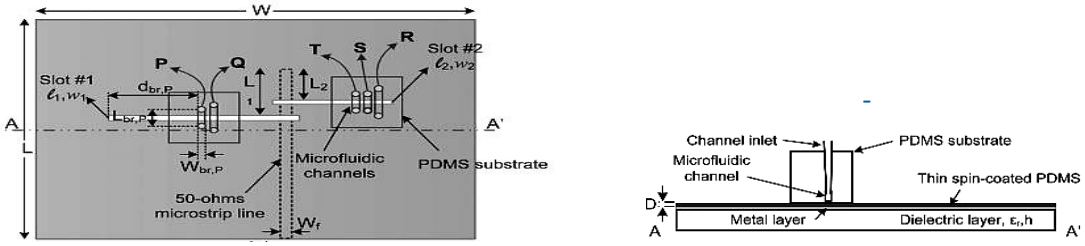

(a) (b)

Figure 12. (a) Top view of the proposed switchable dual band slot antenna. (b) A-A′ cross section of antenna [42].

In [38], a patch antenna with Galinstan loading slot using a pair of open-ended fluidic channel is presented, as seen in Figure 13. The pair of open-ended channels is placed directly at the end of the U-shaped slot. Altering the length of the Galinstan filled channel changes the resonant frequency of the antenna. The microfluidic channels, formed as interlocking circles, facilitate the control the resting position of Galinstan. Results indicate that the reactive loading effect from the U-slot and channel structures is capable of bandwidth tuning of up to 11.2 %, between 1.85 and 2.07 GHz.

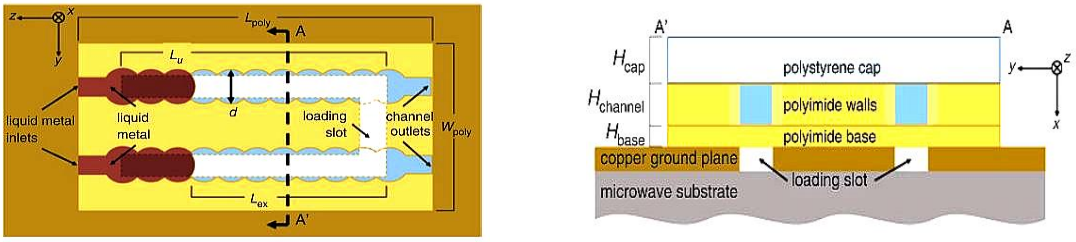

(a) (b)

Figure 13. (a) Frequency-tunable antenna. (b) Cross section of the microfluidic channel structure [38].

Preprints (www.preprints.org) | NOT PEER-REVIEWED | Posted: 9 December 2020 doi:10.20944/preprints202012.0232.v1

3.1.2. Other Frequency Reconfiguration Techniques

Besides the two techniques commonly used for frequency reconfiguration discussed previously, there are several other types of methods which can be used for the same purpose. The first example is the pixelated dipole antenna illustrated in Figure 14 [48]. This antenna is designed based on a baseline planar copper with two side arms. Each arm is replaced by a 1x4 pixel array and is connected to the copper section through a soldered wire. Three additional materials are used to fabricate this antenna; polyimide was used to build the pixel walls, polystyrene as the top cover for the pixel, and PDMS was used as the bottom cover of the pixel array. To connect adjacent pixels, a stainless-steel connector was embedded between the pixel walls. For frequency reconfigurability, these pixels need to be turned on by electrically actuating the Galinstan from the reservoir below the antenna into the pixel. On the contrary, the pixel can be turned off by withdrawing the liquid metal back into the reservoir. This approach resulted in the antenna's switching capability at four resonant frequencies: at 2.51 GHz, 2.12 GHz, 1.85 GHz, and 1.68 GHz, whereas its radiation efficiency ranged from 70.2 % to 75.4 %. Results have also shown that this pixelated antenna did not affect the radiation pattern at the resonant frequencies compared to the measurement of a baseline planar copper dipole.

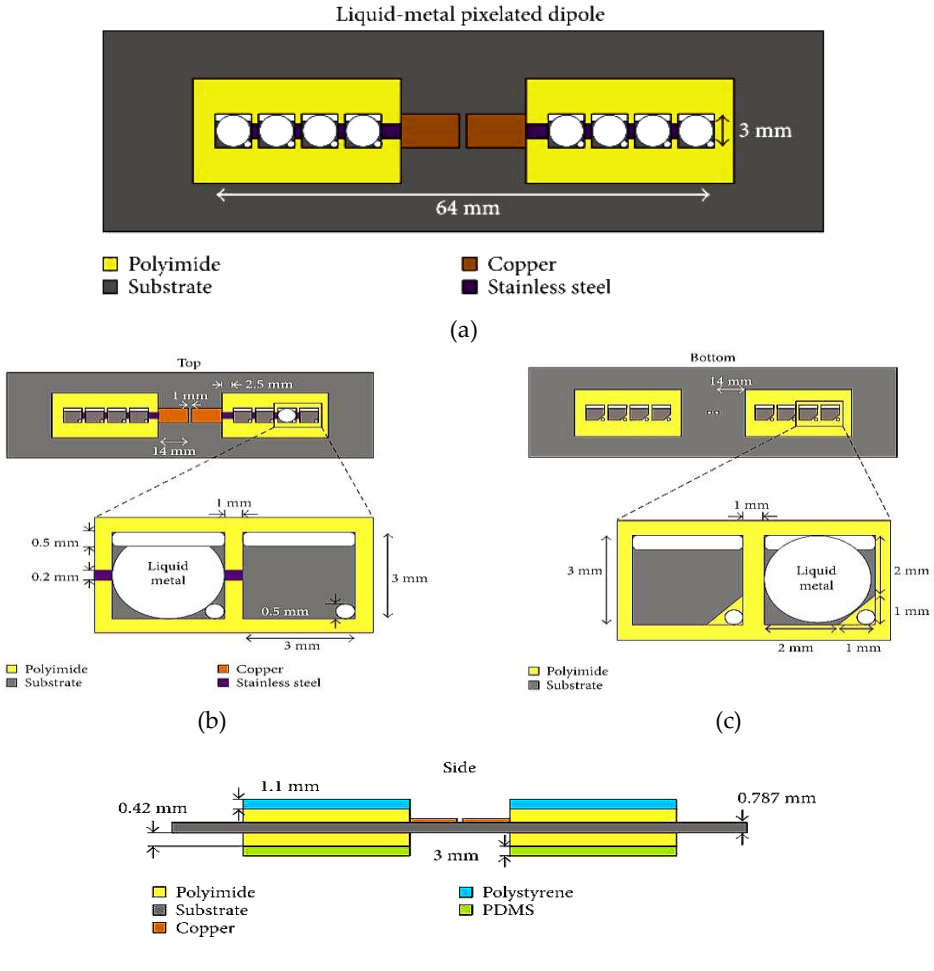

Figure 14. (a) The pixelated dipole antenna. (b) Top side pixel: 'on' state on the left side. (c) Bottom side pixel: 'off' state on the left side. (d) Side view [48].

Next, a frequency-switchable antenna using metallic fluid and vias was presented in [54]. The switchable antenna is designed based on a quarter-mode substrate integrated waveguide (QMSIV)

Preprints (www.preprints.org) | NOT PEER-REVIEWED | Posted: 9 December 2020 doi:10.20944/preprints202012.0232.v1

antenna to be capable of frequency tuning from 3.2 to 4.7 GHz with a frequency switching ratio of 1.45:1. To fabricate the antenna, the printed circuit board (PCB) technology, 3D printing and soft-lithography techniques were utilized to bond the PDMS structure to the circuit board of the QMSIW. This design employed a non-plated through via at the corner of the QMSIW, as shown in Figure 15. The empty via hole enables a resonant frequency of about 3.2 GHz and is increased when it is filled with Galinstan.

In the study presented in [55], a reconfigurable meander antenna was designed to provide operation from 0.5 GHz to 3 GHz. As can be observed in Figure 16, the meander patch is fabricated on top of the substrate, whereas the floating ground plane cavity is located on its reverse side under the meander patch. Galinstan liquid metal is then injected into the cavity of the floating ground plane. The modified floating ground planar which couples to the radiating patch increases the electrical length of the patch. This then leads to frequency reconfigurability with a radiation efficiency of more than 60 %.

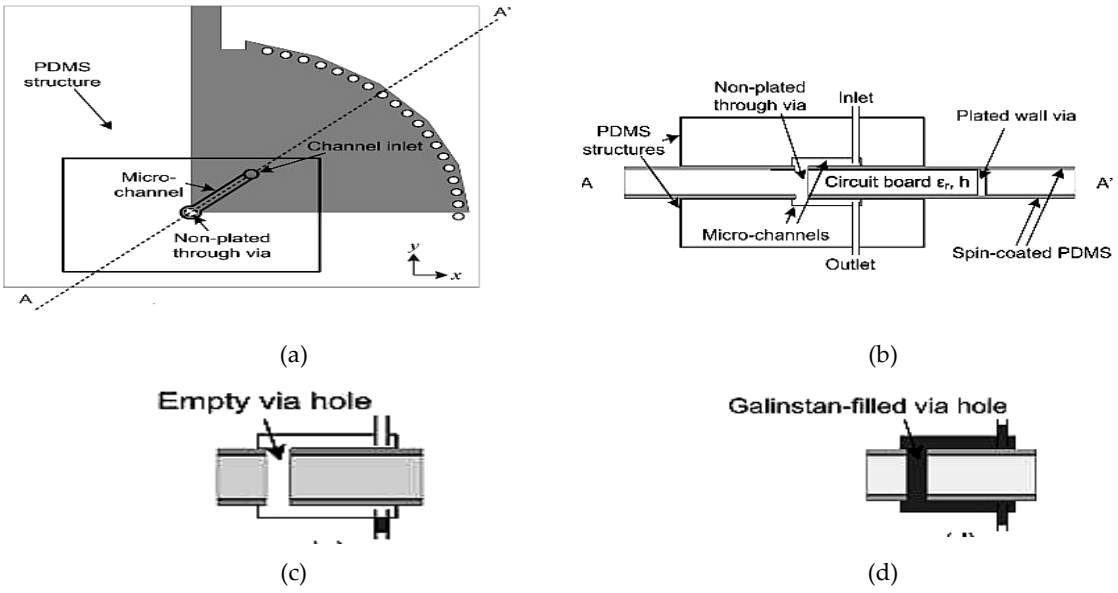

Figure 15. The proposed reconfigurable QMSIW antenna. (a) Top view. (b) A-A′ cross section view. (c)-(d) ON and OFF states of via [54].

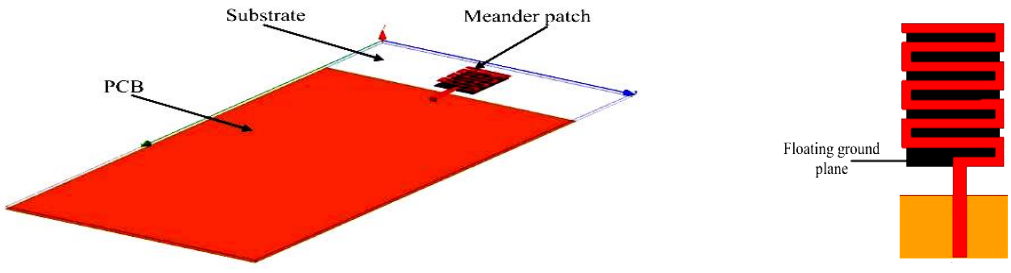

Figure 16. The meander antenna. (a) Perspective view. (b) Meander patch [55].

A summary of frequency reconfigurable antenna techniques using conductive liquids is presented in Table 2.

Preprints (www.preprints.org) | NOT PEER-REVIEWED | Posted: 9 December 2020 doi:10.20944/preprints202012.0232.v1

Table 2. Summary of frequency reconfigurable antennas using non-toxic conductive liquids

Ref	Antenna type	Design approach	Liquid metal type	Frequency range (GHz)	Tuning BW (%)/ tuning ratio	Efficiency (%)
[40]	Slot	Physical/ electrical size modification	Galinstan	1.42 – 1.84	26%	-
[47]	Slot	Physical/ electrical size modification	Galinstan	2.78 – 3.63	36%	-
[16]	PIFA	Physical/ electrical size modification	Galinstan	0.698 – 0.746	-	-
[41]	Slot	Physical/ electrical size modification	EGaIn	2 – 3.5	70%	-
[32]	Shape	Physical/ electrical size modification	Galinstan	2.2 – 9.3	-	-
[52]	Double patch	Physical/ electrical size modification	Galinstan	14.2 – 15.1	-	-
[53]	Loop	Physical/ electrical size modification	Galinstan	0.868 – 2.45 1.7 – 1.9	-	-
[17]	Slot	Reactive loading of liquid metal	Galinstan	2.4, 3.5 and 5.8	>2.5	-
[42]	Slot	Reactive loading of liquid metal	Galinstan	1.8 – 3.1 3.2 – 5.4	1.7:1	78 82
[38]	Slot	Reactive loading of liquid metal	Galinstan	1.85 – 2.07	11.2%	-
[48]	Dipole	Pixelated antenna	Galinstan	1.68, 1.85, 2.12 and 2.51	-	70.2 – 75.4
[54]	QMSIW	Fluidically switched through via	Galinstan	3.2 – 4.7	1.45:1	-
[55]	Meander	Floating ground plane modification	Galinstan	0.5 – 3.9	-	> 60

3.2. Polarization Reconfigurable Antennas

In this section, examples of different types of polarization-reconfigurable antenna will be presented. The approaches employed include the use of dielectric resonator antennas (DRAs), antipodal dipole antennas, slotted antennas, truncated-corner patches and annular antennas.

In [22], a polarization reconfigurable antenna using glass dielectric resonator filled using liquid metal as polarizer is proposed, as seen in Figure 17. This 2.4 GHz antenna is designed to obtain three different states of polarization at the *y*-axis: -45°, +45° and 0° at 2.4 GHz. A glass

Preprints (www.preprints.org) | NOT PEER-REVIEWED | Posted: 9 December 2020 doi:10.20944/preprints202012.0232.v1

DRA is mounted above a ground plane incorporating an aperture. Electric field is coupled from a microstrip transmission line, flows through the aperture and into the DRA, thus polarizing the antenna along the y-axis. Next, the liquid metal is injected into the glass DRA to distribute the electromagnetic field from the y-axis to the angle α. The liquid-metal polarizer rotates the angle of the electromagnetic field clockwise, as shown in Figure 17(e). This design offers a wide effective bandwidth of 18 % and a high radiation efficiency of more than 80 %.

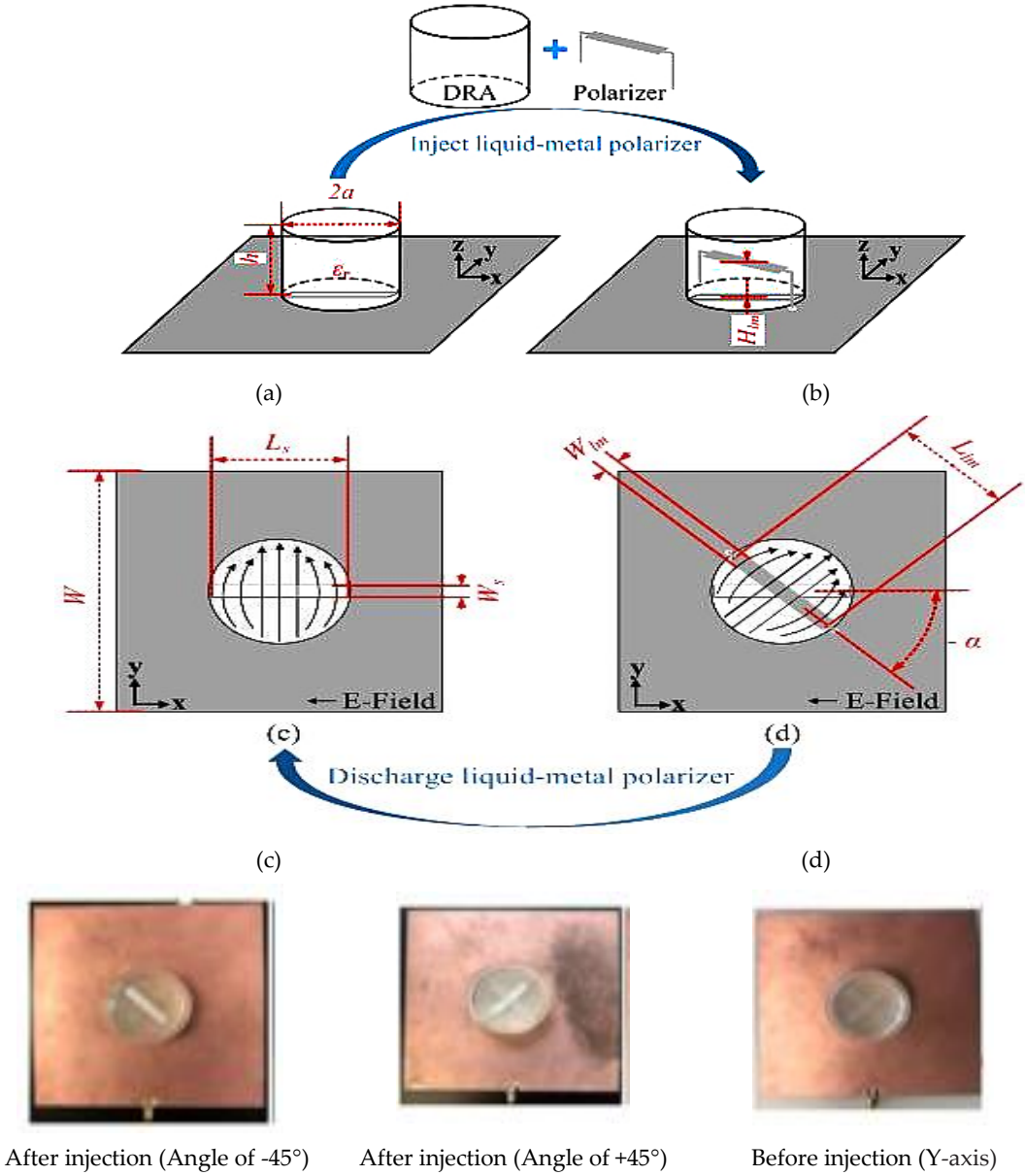

Figure 17. Design principles of the proposed DRA in [22]: (a) DRA without polarizer (b) DRA with polarizer (c) Distribution of electric-field into DRA (d) Distribution of electric-field into DRA with polarizer, and (e) Working angle before and after the liquid-metal injection.

Next, a liquid DRA with radiation efficiency of more than 70% is designed for polarization reconfigurability, as shown in Figure 18 [56],. Ethyl acetate and Galinstan is used as the liquid dielectric solution and liquid-metal solution, respectively. The electric field of the main radiator (formed using the liquid DRA) is excited by an aperture, thus orientating it along the y-axis. Injection

Preprints (www.preprints.org) | NOT PEER-REVIEWED | Posted: 9 December 2020 doi:10.20944/preprints202012.0232.v1

of the liquid metal into the liquid DRA will rotate the electric field from the *y*-axis towards 45° at 2.4 GHz, as shown in Figure 18(b) and (c).

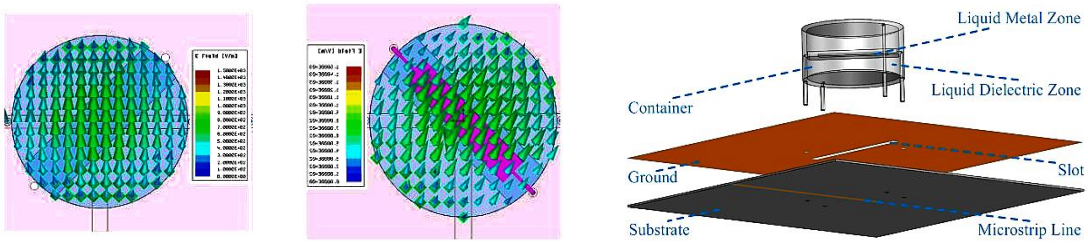

(a) (b) (c)

Figure 18. (a) Antenna structure. (b) Electric field of the DRA without the liquid metal. (c) Electric field of the DRA with the liquid metal [56].

Another antenna proposed in [45] provides polarization reconfigurability using an antipodal dipole antenna, as shown in Figure 19. The antenna polarization can be switched using low power electrical actuation of the liquid metal into states 1, 2 and 3. The states enable the antenna polarization to be oriented +45° to the feed, -45° to the feed or off state, respectively. The applied positive and negative voltage is used to actuate the liquid metal into state 1. Conversely, this voltage difference will be minimal once the liquid metal has arrived at the notches in the channels. Reversing the applied voltage releases the metastable locking and the liquid metal will return into the reservoir. Metastable locking is used to maintain the operating state without the continuous application of voltage. Furthermore, the compact channels can reduce the effect of the electrolyte on the antenna radiation. The maximum gain that can be achieved is between 1.8 and 2.3 dBi with the electrolyte solution, and between 2.4 and 3.0 dBi without the electrolyte.

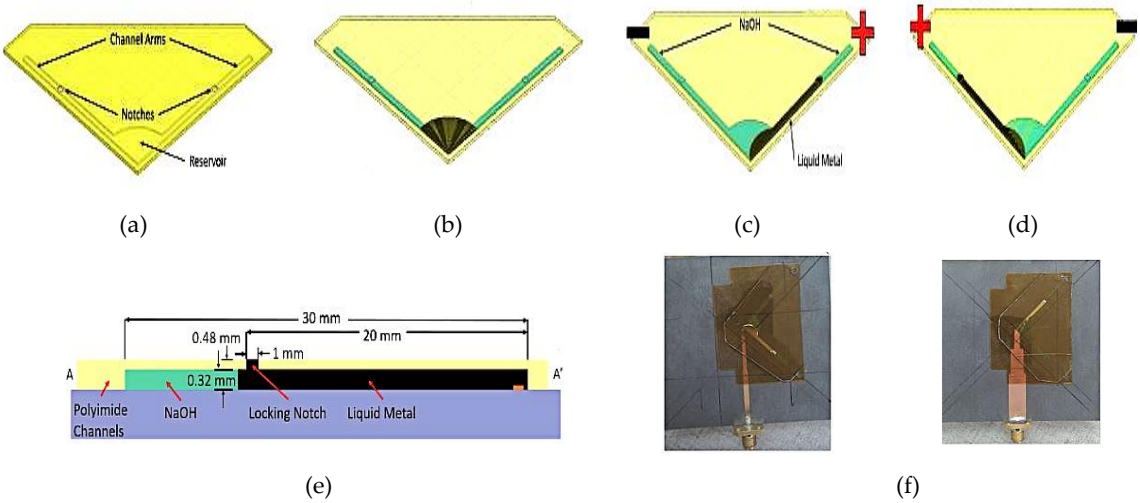

(a) (b) (c) (d) (e) (f)

Figure 19. Liquid metal actuation within the fluidic channels for the antenna in [45]: (a) One-sided channel structure. (b) State 1 with liquid metal (black) and electrolyte solution (green) in the channels. (c) Withdrawing the liquid metal into reservoir. (d) Reversing the polarity to actuate the liquid metal into State 2. (e) The cross section of each arm structure. (f) Front and back of the assembled antenna.

Another approach presented in [23] offered high radiation efficiency of more than 90 % by employing elastomer and minimum use of liquid metal. Different polarization states such as linear polarization (LP), left-hand circular polarization (LHCP) or right-hand circular polarization (RHCP)

Preprints (www.preprints.org) | NOT PEER-REVIEWED | Posted: 9 December 2020 doi:10.20944/preprints202012.0232.v1

can be switched at 2.45 GHz by controlling the location of liquid metal in the four cavities. Standard printed circuit board is used to fabricate the bottom layer of the antenna, whereas the upper layer employed soft lithography technique to mould the cavities into the desired shapes. A truncated-corner square patch was selected to be fabricated using copper tapes and placed on the substrate, whereas Ecoflex is bonded with polyethylene terephthalat (PET) film and is placed conformal to the substrate to form the cavities (Figure 20).

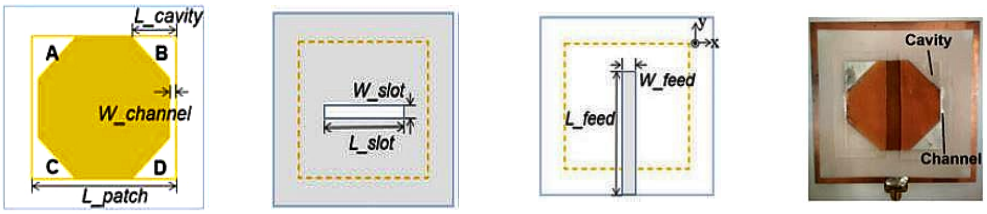

(a) (b) (c) (d)

Figure 20. Schematic of antenna proposed in [23]: (a) upper layer (b) top view (c) bottom view of the lower layer (d) top view of fabricated antenna.

On the other hand, a pressure-actuated switching mechanism is presented in [57] where EGaIn liquid metal was used to change the polarization of two types of antennas. To demonstrate switchable capability between LP and CP, pneumatic actuation is applied onto a: (i) truncated-corner patch antenna; and (ii) an annular slot antenna, as shown in Figure 21. To contain the liquid, PDMS is bonded to a Rogers 4003 substrate whereas two liquid metal channels and two air channels are integrated with the structure. In first antenna, EGaIn is used to perform the polarization switching in the truncated-corner patch antenna. The pressure actuation of the two fluidic metal switches offers a direct connection between patch and the parasitic elements located at the corners, resulting in linear polarization. By releasing the pressure, the liquid metal is retracted to the middle of antenna, thus producing circular polarization. Meanwhile, in the second antenna designed based on an annular slot, the shorting across the slotline generates the linear polarization, whereas retracting the liquid metal into the reservoir generates the circular polarization.

(a) (b)

Figure 21. (a) Truncated-corner patch antenna. (b) Annular slot antenna [57].

In [58], a polarization reconfigurable antenna consisting of a slot antenna and metasurface is proposed. Reconfigurability is enabled by integrating a 4x4 metasurface array as the superstrate of the slot antenna. This metasurface which is made using dielectric substrate is injected with liquid metal to to produce LP, RHCP and LHCP, as depicted in Figure 22. Such approach can provide a good radiation efficiency of about 75%, is low cost and low profile.

Preprints (www.preprints.org) | NOT PEER-REVIEWED | Posted: 9 December 2020 doi:10.20944/preprints202012.0232.v1

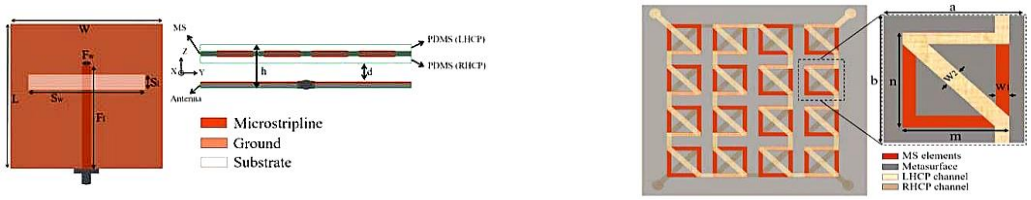

(a) (b)

FIGURE 22. Illustration of the: (a) slotted antenna layout and (b) metasurface layout [58].

Another example of polarization reconfigurable antenna is a E-shaped slotted patch antenna with an extended patch antenna presented in [41], as illustrated in Figure 23. The microfluidic channels are integrated onto the top of the main patch and are allowed to flow between the slot of the main and extended patches to produce different polarization states; RHCP, LHCP and LP. To control the orientation of the LP waves, the length of the microfluidic channel L_{lm1} and L_{lm2} is tuned. The liquid metal can also be switched from L_{lm1} to the other parallel slots to obtain a 180° polarization state. For this method, a radiation efficiency of 99.8 % was achieved.

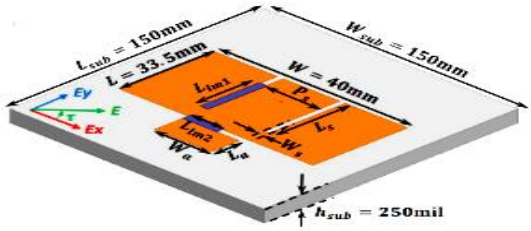

Figure 23. Extended E-shaped patch antenna [41].

A summary of the polarization reconfigurable antennas using conductive liquid metals is presented in Table 3.

3.3 Other Reconfigurations

3.3.1 Gain and Directivity Reconfigurable Antennas

Gain reconfigurability can be enabled by electrically actuating liquid metal using the CEW technique, as seen in [25]. The *X*-mm offset state is the midpoint of the liquid metal slug positioned at *X* mm from the right of the microstrip feed line, as shown in Figure 24. The stub filled with Galinstan liquid metal is reconfigured in terms of length, and consequently tuning the gain of antenna. This 5 GHz antenna provides analogue gain tuning from -5.90 to 4.43 dB. However, this type of antenna is unable to hold the liquid metal in place against unintentional movements.

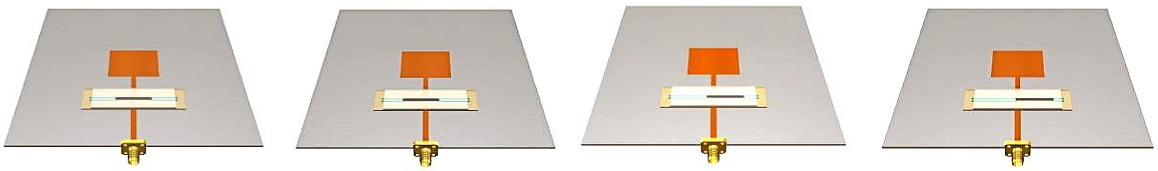

(a) 0 mm offset state (b) 2 mm offset state (c) 5 mm offset state (d) 7 mm offset state

FIGURE 24. States of the Galinstan slug. (a) 0mm offset state. (b)–(d) *X*-mm-offset state [25].

Preprints (www.preprints.org) | NOT PEER-REVIEWED | Posted: 9 December 2020 doi:10.20944/preprints202012.0232.v1

Table 3. Summary of polarization reconfigurable antennas using non-toxic conductive liquid

Ref	Antenna type	Design approach	Conductive liquid metal type	Frequency range (GHz)	Tuning characteristics/ tuning ratio	Efficiency (%)
[22]	DRA	Glass DRA incorporating liquid metal polarizer	Galinstan	2.4	±45°, 0°	> 80
[56]	DRA	DRA incorporating liquid metal	Galinstan	2.4	45°	>70
[45]	Antipodal Dipole	Antipodal dipole with v-shaped channel	Galinstan	3	±45°	-
[23]	Aperture coupled patch antenna	Truncated corner square patch with four triangle cavities of liquid metal	EGaIn	2.45	LHCP, RHCP, LP	>90
[57]	Truncated-corner patch antenna, Annular slot antenna	Truncated at two orthogonal of square patch, Two discontinuities at 45° and 225° across the slotline	EGaIn	2.5	LP, CP	-
[58]	Slot antenna	Slot antenna with metasurface on top of antenna	EGaIn	2.4	LP, RHCP, LHCP	75
[41]	Slot antenna	Rectangular patch with two asymmetrical slot and extended patch slot	EGaIn	2.4	LP, RHCP, LHCP	99.8

Next, a reconfigurable helical antenna is presented, as shown in Figure 25 [59]. This helical antenna is tuned by filling the 3D printed helical channels with EGaIn. The antenna gain is determined by the number helical turns, and this in turn, is controlled by the volume of EGaIn

Preprints (www.preprints.org) | NOT PEER-REVIEWED | Posted: 9 December 2020 doi:10.20944/preprints202012.0232.v1

inserted into the channels. Increasing the number of helical turns from 2 to 8 increases the gain from about 5 to 9 dBi at 5 GHz.

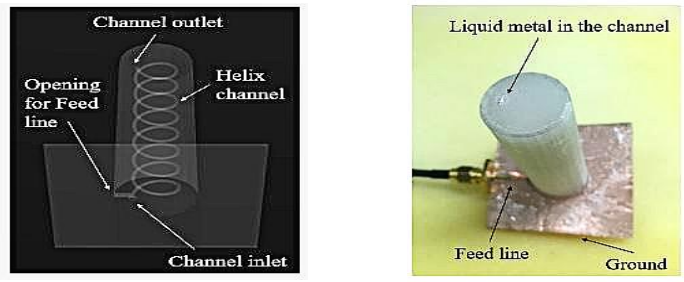

(a) (b)

Figure 25. Fabricated prototype. (a) Photograph of antenna. (b) Proposed antenna [59].

On the other hand, directivity reconfiguration can be achieved using a two-arm spiral antenna [24]. EGaIn liquid metal is encased into a stretchable silicone elastomer to form a wideband antenna, as seen in Figure 26. By increasing the height of elastomer inflation using a microblower, the *y*-direction (90°) will be increased, and the radiation along -*y*-direction (270°) will decrease simultaneously, thus optimizing the directivity of main lobe (in the *y*-direction). This antenna generates a circular polarization and enables wideband frequency operation from 6.9 to 13.8 GHz with radiation efficiency from 60.5 to 72 %.

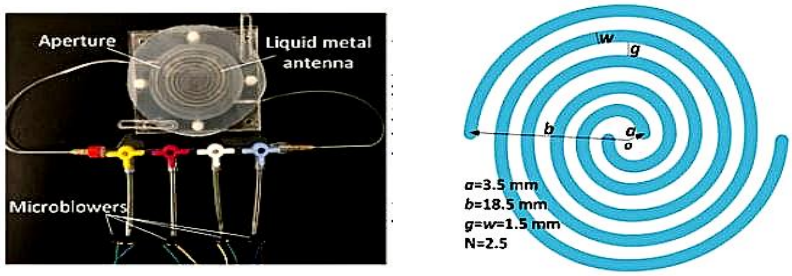

(a) (b)

Figure 26. (a) The directivity-reconfigurable wideband antenna assembly. (b) Design parameters of the two-arm spiral antenna [24].

3.3.2 Phase Reconfigurable Antenna

Besides gain, the phase of an antenna can also be reconfigured using liquid metal. One of the first research presenting such reconfigurability is a microfluidic transmitarray unit cell presented in [60]. Continuous phase shifting is achieved using the element rotation method. The unit cell consists of a double-layered nested ring-split ring structure implemented in the form of microfluidic channels, and are integrated within a PDMS substrate, as shown in Figure 27. Galinstan is injected into the rings to form the conductive regions, whereas the split regions are air-filled. Moving the liquid metal around the ring along the split offers a 360° range of linear phase shift through the unit cell in the transmitted field. Its main advantage is that each unit cell can be easily controlled by a pair of tubes attached to a micropump.

Preprints (www.preprints.org) | NOT PEER-REVIEWED | Posted: 9 December 2020 doi:10.20944/preprints202012.0232.v1

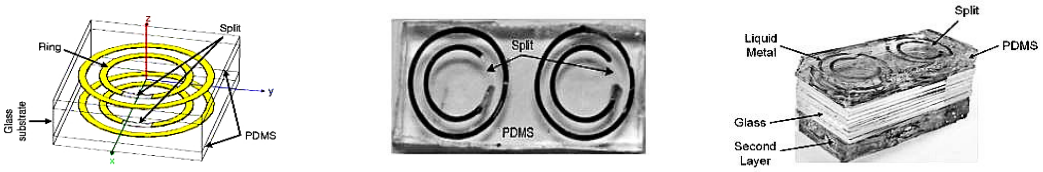

(a) (b) (c)

Figure 27. Unit cell of the nested ring-split ring transmitarray. (a) Double layered. (b) One layer for the rotation angle of 20°. (c) Fabricated double layered antenna [60].

3.3.3 Compound Reconfigurable Antennas

There are various enabling technologies to combine two or more parameters reconfiguration in an antenna. They may differ significantly in terms of spectral efficiency, performance, or other characteristics such as integration and compactness.

The first example of such compound reconfigurable antenna is presented in [46], where the antenna is capable of polarization and pattern reconfigurability using ECA. Five discrete phase shift states can be provided, i.e. at 0°, -45°, 45°, -90° and 90° to enable polarization reconfigurability and null directions. To obtain X° configuration, the liquid metal is electrically actuated into the (colored) fluid arms enclosed by polyimide fixture (grey), as shown in Figure 28. This antenna achieved a radiation efficiency ranging from 69 % to 97 %. On the other hand, the local polyimide-built surface energy is used to enable metastable locking, which is needed to maintain each state.

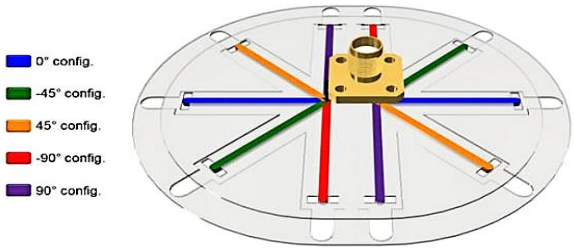

Figure 28. Polarization and pattern reconfigurable dipole antenna [46].

Next, a crossed dipole with reconfigurable frequency and polarization is proposed in [14]. It comprises of four glass capillaries designed in an acrylic fixture, as shown in Figure 29. Six laser-cut cavities in the acrylic fixture form two central liquid metal reservoirs and four outer electrolyte reservoirs to support both ends of the capillaries. DC voltage is used to shorten and lengthen the liquid metal in the capillaries to implement the ECC technique. The multidirectional spread of the liquid metal changes the length of the dipole arms to generate the linear and switchable linear (0.8 – 3 GHz) to circular polarization (0.59 – 1.63 GHz) with radiation efficiency ranging from 41 % to 70 %, similar to [21].

Besides that, a pattern and polarization-reconfigurable helical antenna using mechanically-actuated liquid metal is presented in [44], as shown in Figure 30. The antenna comprises of a helical structure made using a polymer tube, which is wound around a Acrylonitrile Butadiene Styrene (ABS) fixture. Galinstan liquid metal is pumped into the polymer tube using a Raspberry Pi-controlled micropump. This 1.575 GHz antenna generated four beams: circularly- and elliptically-polarized axial beams, and linearly-polarized semi-doughnut and axial beams.

Preprints (www.preprints.org) | NOT PEER-REVIEWED | Posted: 9 December 2020 doi:10.20944/preprints202012.0232.v1

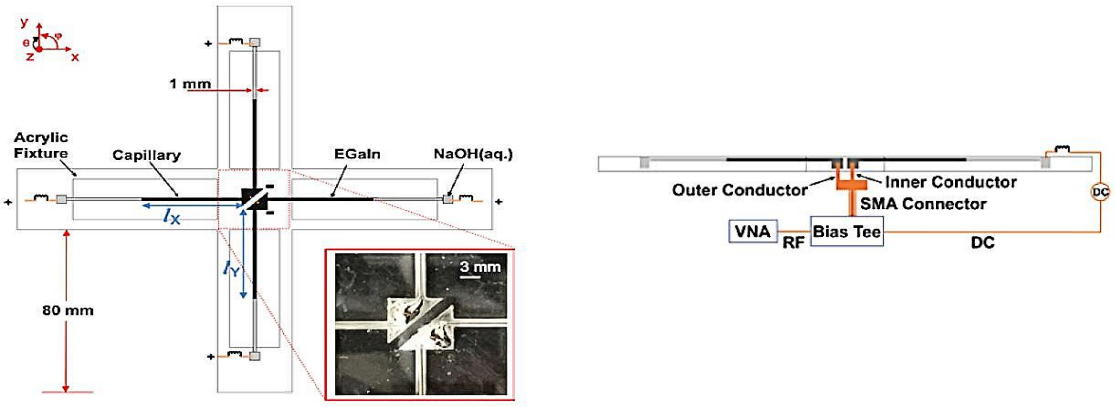

(a) (b)

Figure 29. Schematic of the: (a) Reconfigurable crossed dipole, and (b) Feed detail [14].

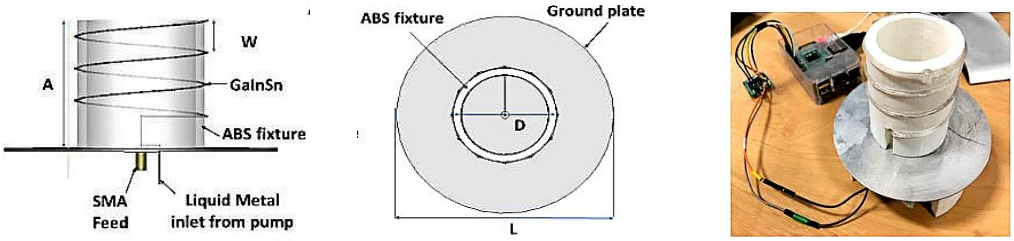

(a) (b) (c)

Figure 30. The proposed antenna in [44]: (a) Side view (b) Top view, and (c) Antenna prototype.

In [61], a 3D printed 'tree' antenna was designed for frequency, polarization and radiation pattern reconfiguration. A zig-zag antenna and a helical antenna are integrated into a zipper origami Voronoi structure, which is used as the scaffolding structure to mechanically tune the radiation pattern and to minimize the storage requirement, as shown in Figure 31. EGaIn liquid metal is used to switch between the two antennas and to allow flexible implementations. The compression of this 'tree' (zig-zag and helical) antenna is capable of producing a dual band operation in the 3G and 5G bands, with dual polarization and with directional and omnidirectional radiation patterns. Antennas implementing conductive liquid for other types of reconfiguration are summarized Table 4.

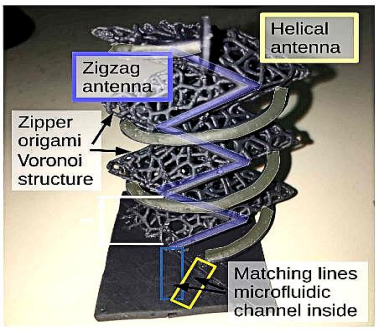

Figure 31. 3D printed antenna tree [61].

Preprints (www.preprints.org) | NOT PEER-REVIEWED | Posted: 9 December 2020 doi:10.20944/preprints202012.0232.v1

Table 4. Summary of antennas with other types of reconfiguration using non-toxic conductive liquids

Ref	Antenna/ Liquid metal type	Design approach	Reconfiguration type	Frequency range (GHz)	Tuning characteristics	Efficiency (%)
[25]	Patch antenna/ Galinstan	Rectangular patch with inset feed line and copper stub	Gain	5	-5.90 – 4.43 dB	-
[59]	Helical antenna/ EGaIn	Helical antenna with 8 turns	Gain	5	> 4 dBi	-
[24]	Two-arm spiral antenna/ EGaIn	Spiral antenna is embedded into silicone elastomer	Directivity	6.9 – 13.8	*y*-direction (90°) and -*y*-direction (270°)	60.5 - 72
[60]	Transmitarray unit cell/ Galinstan	Unit cell with split ring structure	Phase	8 – 10	360° linear phase shift	-
[46]	Dipole antenna/ Galinstan	Dipole arms containing liquid metal are enclosed into Polyimide fixtures	Compound (polarization and pattern)	1.579	0°, -45°, 45°, -90° and 90°	69 - 97
[14]	Crossed-dipole antenna/ EGaIn	Crossed dipole with two pairs of dipole arms	Compound (frequency and polarization)	0.8 – 3	LP (0.8 – 3) CP (0.89 – 1.63)	41 – 70
[44]	Helical antenna/ Galinstan	Helical turns made using flexible polymer tube containing liquid metal	Compound (pattern and polarization)	1.575	CP and EP axial beams, LP semi-doughnut and axial beams	-
[61]	Origami antenna/ Galinstan	Origami with zig-zag and helical shaped	Compound (frequency, polarization and pattern)	3 and 5	3 to 5 GHz LP to CP, Directional to omnidirectional	-

4. Reconfigurable Antennas Using Other Liquids

In this section, reconfigurable technologies using other liquids that enables frequency, polarization and pattern reconfiguration will be presented. The first is a microfluidically-reconfigurable frequency-tunable monopole antenna using mercury as conductive liquid presented

Preprints (www.preprints.org) | NOT PEER-REVIEWED | Posted: 9 December 2020 doi:10.20944/preprints202012.0232.v1

in [43]. The antenna is implemented by stacking the substrate containing the liquid metal forming a monopole antenna, as shown in Figure 32. The microfluidic channel is fabricated within a PDMS substrate using the lithography process and is sealed using liquid crystal polymer (LCP) substrate. This channel is aligned with the microstrip feedline to generate capacitive coupling through the LCP layer. The LCP layer is then bonded to a Rogers RT5880 substrate consisting of a microstrip line and a ground plane. A bidirectional micropump was used to move the liquid metal on the microstrip feed line, which then reconfigures the physical length of the antenna. Prior to that, a syringe was used to inject the mercury and Teflon solutions inside the microfluidic channel. The choice of mercury is due to its low rate stiction and oxidation properties. This antenna provided a frequency tuning range from 1.29 to 5.17 GHz. The proposed antenna can also be used to form a monopole array antenna capable of frequency tuning from 2.5 to 5 GHz with radiation efficiency of 80 % and 65 %, respectively.

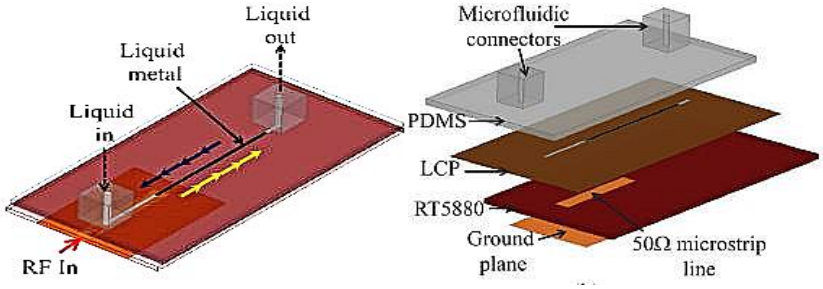

Figure 32. Substrate stack-up of the liquid-metal monopole antenna [43] .

Next, a fluidically-switched Vivaldi antenna using ionized water was proposed in [62], which operation can be tuned between the 3.2 GHz and 4.5 GHz band. A microstrip feed line with an open circuit stub is fabricated on the top layer of the substrate, as illustrated in Figure 33. The feed line couples the signal to the slot line on the bottom layer. The conductive fluid switch enclosure contains deionized water dissolved using 2 mol of Potassium Chloride (KCI) solution. Operation in the higher frequency band of 4.5 GHz can be achieved by pumping the conductive fluid into the switch to shorten the current patch, whereas draining out the fluid enables operation at 3.2 GHz with an efficiency of 87%.

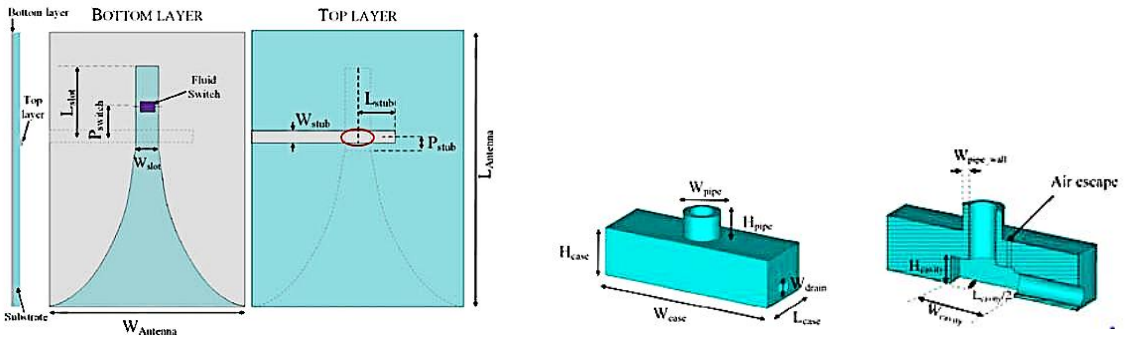

(a) (b) (c)

Figure 33. (a) Bottom and top layer of the fluidically-switched antenna. (b) Fluid switch. (b) cross sectional view of the fluid switch [62].

In [63] a frequency reconfigurable planar antenna using castor oil and ethyl acetate as its dielectric fluid has been proposed, as illustrated in Figure 34. A sealed plastic enclosure box is used to provide very good electrical isolation between the control circuitry and the antenna made using

Preprints (www.preprints.org) | NOT PEER-REVIEWED | Posted: 9 December 2020 doi:10.20944/preprints202012.0232.v1

copper sheet. This plastic enclosure is made using ABS (for its body) and clear polycarbonate (for its lid). The bent dipole antenna is placed on the inner sides of the ABS enclosure. A flexible diaphragm comprising of a latex rubber sheet is placed across the opening of the sealed box. Pumping of the cavity from the polycarbonate side (behind the antenna) will bind the dielectric fluid onto the upper boundary of the flexible diaphragm, thus changing the resonant frequency. To feed the antenna, a coaxial cable is inserted into the cavity, with the inner conductor is soldered to point A, whereas the coaxial shielding is connected to point B. A gamma matching section made using ferrite beads (denoted as sections C and D) is designed to act as a choke to stop the unbalanced current from flowing down the cable. By using two dielectric fluids (castor oil and ethyl acetate), a tuning range of 25 % (from 1.17 to 1.5 GHz) and 46 % (from 0.9 to 1.44 GHz) can be achieved. This comes at a cost of a decrease in efficiency to 48% and 25%, respectively, in each operating band.

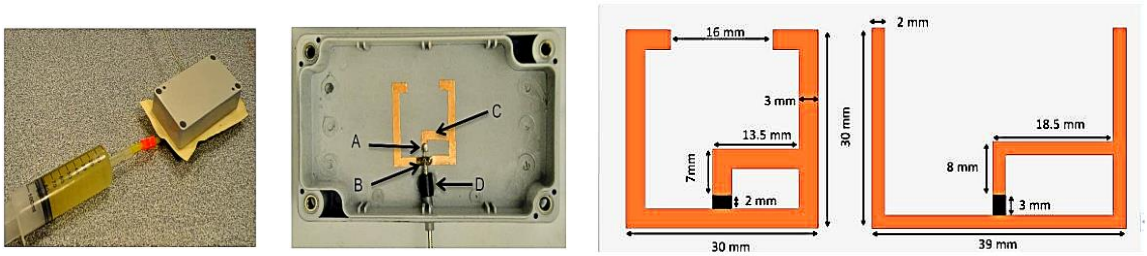

(a) (b) (c)

Figure 34. (a) Plastic antenna box, latex diaphragm and syringe. (b) Bent dipole antenna and coaxial cable arrangement. (c) Dimensions of the two bent dipole antennas with castor oil (on the left) and ethyl acetate (on the right) [63].

Another example of a frequency reconfigurable patch antenna is one using deionized (DI) water placed in microfluidic channels, as proposed in [64]. Figure 35 illustrates the topology of the antenna, consisting of two Rogers 4003C substrates and polypropylene tubes acting as the microfluidic channels. The patch is designed on top of substrate A, while the copper on top of substrate B acts as ground plane. The tubes are symmetrically placed between substrate A and the ground. A micropump is used to pump the DI water in or out of the tubes. The tuning range, states and frequencies are realized by adjusting the number and location of the tubes. It is operated based on the changes in effective dielectric constant value between the regions of patch and ground plane. The operating frequency without the tubes is 2.04 GHz, whereas insertion of the two pair of tubes achieved a tuning frequency from 1.391 to 1.861 GHz with efficiency more than 68.8 %.

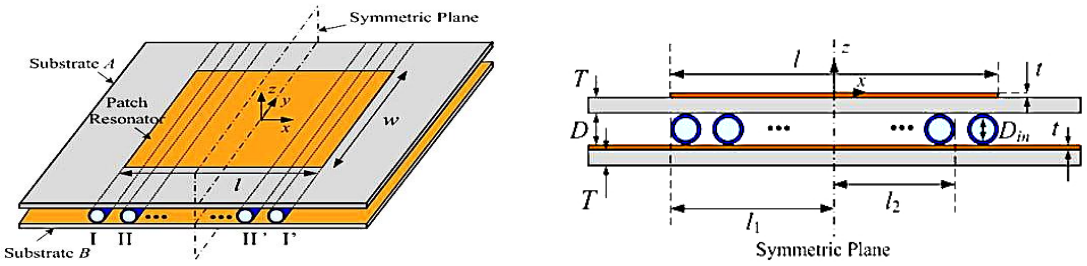

(a) (b)

Figure 35. Microfluidic frequency reconfigurable patch antenna. (a) 3D view. (b) Side view [64].

In the study in [65], an antenna with circular polarization reconfigurability is proposed using a truncated liquid DRA. This antenna is designed for operation in the 2.4 GHz band for RFID applications. It is fed using a single probe and is integrated onto two arbitrary sides (left and right

Preprints (www.preprints.org) | NOT PEER-REVIEWED | Posted: 9 December 2020 doi:10.20944/preprints202012.0232.v1

zones) of a 3D-printed container, as depicted in Figure 36. The polarization switching states can be changed by pumping the dielectric fluid (ethyl acetate) solution into the left or right section, resulting in a LHCP or RHCP, respectively. The proposed antenna achieved an efficiency more than 70 %, a wide operating bandwidth of 35.6 % (from 2.08 to 2.98 GHz) and an axial ratio (AR) bandwidth of 16.3% (from 2.31 to 2.72 GHz).

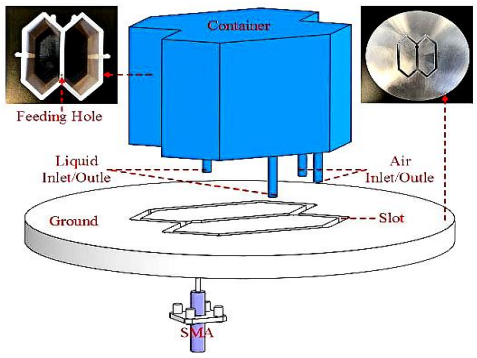

Figure 36. Liquid DRA [65].

Next, the application of a dielectric fluid to achieve pattern reconfigurability using a tunable DRA is presented in [66]. The antenna made using two DRAs are illustrated in Figure 37. The glass cylinder represents as static inner zone of the DRA, whereas the outer zone is a liquid-based cylindrical DRA. A 3D-printed container is used to cover both DRAs, and both structures are fed using a coaxial probe. When dielectric fluid (ethyl acetate) is pumping in and out of the outer zone, the reconstituted DRA is excited in the conical transverse magnetic ($TM_{01\delta}$ mode) with 50 % to 60 % of radiation efficiency. On the other hand, the glass DRA is excited in a broadside hybrid electromagnetic $HEM_{11\delta}$ mode with an efficiency more than 80 %. Manipulating both DRA modes enables radiation pattern reconfigurability over a wide impedance bandwidth of 35 %, with its operating frequency ranging from 3.75 to 5.37 GHz. The liquid-based antennas using other liquids have been summarized in Table 5.

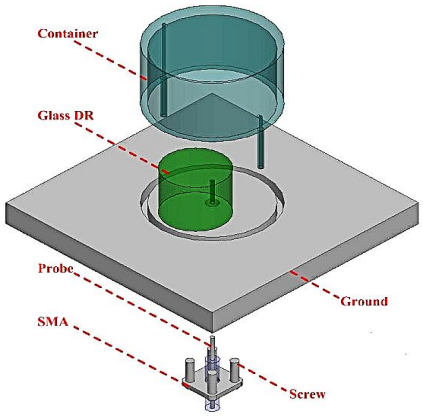

Figure 37. Reconfigurable DRA presented in [66] .

Preprints (www.preprints.org) | NOT PEER-REVIEWED | Posted: 9 December 2020 doi:10.20944/preprints202012.0232.v1

Table 5. Summary of reconfigurable antennas using other conductive and dielectric liquids

Ref	Antenna/ Liquid type	Design approach	Reconfiguration type	Frequency range (GHz)	Tuning characteristics/ tuning ratio	Efficiency (%)
[43]	Monopole antenna/ Conductive (mercury)	Monopole with capacitive coupling feed line	Frequency	2.5 to 5	~ 4:1	80, 65
[62]	Vivaldi antenna/ Conductive (EGaIn)	Feed line coupled to slot line	Frequency	3.2 and 4.5	-	87
[63]	Dipole antenna/ Dielectric (castor oil and ethyl acetate)	Two bent dipoles with plastic enclosure	Frequency	1.17 – 1.50 0.9 to 1.44	25% 46%	90 – 47, 92 – 82
[64]	Microfluidic microstrip patch/ Dielectric (DI water)	Inserting liquid tubes between the patch and the ground plane	Frequency	1.391 – 1.861	-	68.8 – 86.3
[65]	DRA/ Dielectric (ethyl acetate)	Container with left and right rectangular sections	Polarization	2.4	LHCP (16.7%), RHCP (16.3%)	> 70
[66]	DRA/ Dielectric (ethyl acetate)	DRA with inner and outer sections	Pattern	3.75 – 5.37	$HEM_{11\delta}$ mode (outer section empty) TM01δ (outer section full)	> 80, 50 - 63

5. Future Perspectives

There are several practical considerations in maintaining and improving the performance of reconfigurable antennas using liquid metal. Some of the consideration are suggested in this section, based on the findings of the literature. The most prominent limitation of the liquid metal is the possibility of the oxidation layer build-up caused by the use of gallium-based liquid metal such as Galinstan and EGaIn. An effective solution in alleviating this is the electrolyte solution. In addition to this, there are still challenges with the commonly used actuation methods such as ECA, CEW and ECC. They include the need for a suitable supporting electrolyte. Therefore, studies related to the viscosity level of acids, alkaline and bases must be performed to ensure its appropriate level to

 doi:10.20944/preprints202012.0232.v1

continually prevent the creation of the oxidation layer. Liquid metal is also susceptible to the corrosive effect of the copper probe. Thus, the actuating probe must be chosen with care to ensure its resistance to alkaline or acids corrosion. Finally, studies also must be conducted to evaluate the life expectancy of metal fluids and electrolytes. This is to minimize the effects of the liquid metal oxidation, ensuring stable antenna performance and extending the life expectancy of the antenna.

6. Conclusions

This manuscript reviewed the current state-of-the-art in liquid metal-based reconfigurable antennas. Reconfiguration of antenna parameters (such as frequency, polarization, gain, directivity, phase shifting or their combinations) can be achieved by controlling the injection of liquid metal into microfluidic channel to alter the physical size of antenna. The implementation of capacitive or reactive loading also can reduce the physical size of antenna, at the cost of antenna efficiency. Besides that, the use of lossy material such as PDMS also affects antenna efficiency. Straight fluidic channels have been mainly used to simultaneously ensure robustness of the antenna and to enable gradual tuning which then improves the positioning accuracy of the liquid. However, channels with notches or interlocking circles are required to maintain the liquid metal in position against any antenna tilting or unintentional motions. On the contrary, open ended fluidic channels must be avoided as they do not securely maintain the liquid metal in the channel, is prone to leakage and will reduce antenna robustness.

From these recent literatures, planar antennas are the most widely used antenna as frequency reconfigurable antennas. Such antenna types include the slotted antennas, PIFAs, planar patches, pixelated dipoles, switchable QMSIV and meandered patch antennas. In addition to that, loop antennas which uses fluidic tubes is another viable alternative. On the other hand, polarization reconfiguration is achieved using antipodal dipole antennas, truncated-corner patches, slotted antennas and annular antennas. Besides that, the concepts of DRAs in enabling polarization reconfiguration is also presented and discussed. Meanwhile, gain and directivity reconfiguration can be achieved by either tuning the length of the matching stub, or by tuning the orientation of the unit cell in a metasurface superstrate. For the former, a two-arm spiral antenna is designed on a stretchable silicone elastomer to obtain directivity reconfigurability, whereas the use of tunable unit cell can result in phase shifting for a transmitarray. The final category, which is the compound reconfigurable antenna can be implemented in practice by using dipole, crossed dipole, helical or zig-zag antennas. These antennas are capable in reconfiguring two or more antenna parameters (frequency, polarization, gain, phase, etc) instead of a single parameter.

It can be summarized that there exist three methods can be used to control liquid flow and consequently reconfigure the antenna: (i) manual actuation, (ii) pneumatic actuation and (iii) electrical actuation. Generally, syringe is used to manually actuate liquid metal using air pressure. This process can be repeated and reversed by designating the inlet and outlet of the liquid metal separately. However, when using a syringe, additional time is taken for moving the fluid in the channels. Hence, pneumatic actuation via micropump can be used to significantly reduce this duration. However, in applications which requires antennas to be compact in size, the use of micropump units is a disadvantage due to the additional space requirement. Furthermore, such technique can be challenging to realize frequency reconfigurable antenna arrays with high gain. For this reason, pump-free electrical potential actuation mechanisms are needed. These mechanisms

 doi:10.20944/preprints202012.0232.v1

include the likes of ECA, CEW and ECC, which require the direct contact of electrolyte with the liquid metal. Bias voltage is supplied using these electrodes to actuate the liquid metal in the intended liquid channels. Conversely, swapping the polarities of the applied voltage will restore the liquid metal to its original position. This technique requires low power in actuating the liquid metal movements in a channel by manipulating its surface tension. Nonetheless, all aforementioned techniques can also be integrated with electrical control in a larger feedback system.

The ECA actuation of liquid metals can be performed by applying a positive DC bias voltage on the electrolyte that surrounds the liquid metal to induce its surface tension. This then moves the liquid metal towards the positive bias. To avoid the liquid metal from withdrawing back to its original position, a continuous bias voltage must be applied. However, the incorporation of the ECA and metastable locking method can be implemented simultaneously to sustain the position of the liquid metal without a continuous bias voltage. In contrast to ECA, the CEW method allows the liquid metal to move from point to point instead of deforming or reshaping. In ECA and CEW approaches, there is no chemical reaction involved in the actuation of liquid metal. However, neutral electrolytes can build up oxide layers and mechanically hinder the movements of liquid metal in these channels. Using the ECC method, excess oxidation layers can be removed using a strong acid or base solutions.

Despite the significant progress in each approach, there are still ample possibilities for future developments and studies. As trade-off typically exists between the material properties of the liquids, types of channels and antenna performance, novel antenna designs, new materials, innovative techniques in liquid metal actuation and antenna fabrication, or any combination of them will continue to attract antenna researchers' attention for years to come.

Funding: This work was supported in part by the Ministry of Education Malaysia under Hadiah Latihan Persekutuan (HLP), and in part by King Mongkut's University of Technology North Bangkok under grant number KMUTNB-64-KNOW-46.

Acknowledgments: The authors would like to extend their appreciation to anonymous reviewers through their valuable feedback and comments, which will greatly improve the content of this manuscript.

Conflicts of Interest: The authors declare no conflict of interest.

References

1. B. Bhellar and F. A. Tahir, "Frequency reconfigurable antenna for hand-held wireless devices," *IET Microwaves, Antennas Propag.*, vol. 9, no. 13, pp. 1412–1417, 2015.
2. J. Costantine, Y. Tawk, S. E. Barbin, and C. G. Christodoulou, "Reconfigurable antennas: Design and applications," *Proc. IEEE*, vol. 103, no. 3, pp. 424–437, 2015.
3. M. S. Khan, B. Ijaz, D. E. Anagnostou, B. D. Braaten, A.-D. Capobianco, and S. Asif, "Frequency reconfigurable self-adapting conformal array for changing surfaces," *IET Microwaves, Antennas Propag.*, vol. 10, no. 8, pp. 897–901, 2016.
4. A. S. Elkorany, S. A. Saad, and D. A. Saleeb, "Compact reconfigurable band notched UWB cylindrical dielectric resonator antenna using single varactor diode," *Adv. Electromagn.*, vol. 7, no. 3, pp. 35–39, 2018.
5. J. M. Floc'H, I. Ben Trad, and I. Rouissi, "Mechanically tunable meander antenna for cognitive radio," *2016 10th Eur. Conf. Antennas Propagation, EuCAP 2016*, 2016.
6. B. Babakhani and S. Sharma, "Wideband Frequency Tunable Concentric Circular Microstrip Patch Antenna with Simultaneous Polarization Reconfiguration," *IEEE Antennas Propag. Mag.*, vol. 57, no. 2, pp. 203–216, 2015.
7. Y. Xu, Y. Tian, B. Zhang, J. Duan, and L. Yan, "A novel RF MEMS switch on frequency reconfigurable

antenna application," *Microsyst. Technol.*, vol. 24, pp. 3833–3841, 2018.

8. S. Cheng and Z. Wu, "Microfluidic electronics," *Lab Chip*, vol. 12, no. 16, pp. 2782–2791, 2012.
9. D. Rodrigo, L. Jofre, and B. A. Cetiner, "Circular beam-steering reconfigurable antenna with liquid metal parasitics," *IEEE Trans. Antennas Propag.*, vol. 60, no. 4, pp. 1796–1802, 2012.
10. S. I. Hussain Shah and S. Lim, "Microfluidically frequency-reconfigurable quasi-yagi dipole antenna," *Sensors (Switzerland)*, vol. 18, no. 9, pp. 1–9, 2018.
11. C. B. Eaker and M. D. Dickey, "Liquid metal actuation by electrical control of interfacial tension," *Appl. Phys. Rev.*, vol. 031103, no. 3, pp. 1–11, 2016.
12. A. Dey, R. Guldiken, and G. Mumcu, "Microfluidically Reconfigured Wideband Frequency-Tunable Liquid-Metal Monopole Antenna," *IEEE Trans. Antennas Propag.*, vol. 64, no. 6, pp. 2572–2576, 2016.
13. M. Wang, M. R. Khan, C. Trlica, M. D. Dickey, and J. J. Adams, "Pump-free feedback control of a frequency reconfigurable liquid metal monopole," *IEEE Antennas Propag. Soc. AP-S Int. Symp.*, vol. 2015-Octob, pp. 2223–2224, 2015.
14. M. Wang, M. R. Khan, M. D. Dickey, and J. J. Adams, "A compound frequency- and polarization-reconfigurable crossed dipole using multidirectional spreading of liquid metal," *IEEE Antennas Wirel. Propag. Lett.*, vol. 16, pp. 79–82, 2017.
15. Y. Zhou, S. Fang, H. Liu, and S. Fu, "A Liquid Metal Conical Helical Antenna for Circular Polarization-Reconfigurable Antenna," *Hindawi Int. J. Antennas Propag.*, vol. 2016, pp. 1–7, 2016.
16. A. Ha and K. Kim, "Frequency tunable liquid metal planar inverted-F antenna," *Appl. Phys. Lett.*, vol. 52, no. 2, pp. 100–102, 2016.
17. A. Pourghorban Saghati, J. Singh Batra, J. Kameoka, and K. Entesari, "Miniature and reconfigurable CPW folded slot antennas employing liquid-metal capacitive loading," *IEEE Trans. Antennas Propag.*, vol. 63, no. 9, pp. 3798–3807, 2015.
18. H. A. Majid and M. K. A. Rahim, "Frequency and pattern reconfigurable slot antenna slot antenna," *IEEE Trans. Antennas Propag.*, vol. 62, no. 10, pp. 5339–5343, 2014.
19. S. Ghosh and S. Lim, "Fluidically reconfigurable multifunctional frequency-selective surface with miniaturization Characteristic," *IEEE Trans. Microw. Theory Tech.*, vol. 66, no. 8, pp. 3857–3865, 2018.
20. L. Song, W. Gao, C. O. Chui, and Y. Rahmat-Samii, "Wideband Frequency Reconfigurable Patch Antenna with Switchable Slots Based on Liquid Metal and 3-D Printed Microfluidics," *IEEE Trans. Antennas Propag.*, vol. 67, no. 5, pp. 2886–2895, 2019.
21. M. Wang, C. Trlica, M. R. Khan, M. D. Dickey, and J. J. Adams, "A reconfigurable liquid metal antenna driven by electrochemically controlled capillarity," *J. Appl. Phys.*, vol. 117, no. 19, pp. 1–5, 2015.
22. Z. Chen, H. Wong, and J. Kelly, "A Polarization-Reconfigurable Glass Dielectric Resonator Antenna Using Liquid Metal," *IEEE Trans. Antennas Propag.*, vol. 67, no. 5, pp. 3427–3432, 2019.
23. C. Wang, J. C. Yeo, H. Chu, C. T. Lim, and Y.-X. Guo, "Design of a reconfigurable patch antenna using the movement of liquid metal," *IEEE Antennas Wirel. Propag. Lett.*, vol. 17, no. 6, pp. 974–977, 2018.
24. P. Liu, S. Yang, X. Wang, M. Yang, J. Song, and L. Dong, "Directivity-reconfigurable wideband two-arm spiral antenna," *IEEE Antennas Wirel. Propag. Lett.*, vol. 16, pp. 66–69, 2017.
25. G. B. Zhang, R. C. Gough, M. R. Moorefield, K. S. Elassy, A. T. Ohta, and W. A. Shiroma, "An Electrically Actuated Liquid-Metal Gain-Reconfigurable Antenna," *Int. J. Antennas Propag.*, vol. 2018, no. 1, pp. 3–10, 2018.
26. M. A. H. Khondoker and D. Sameoto, "Fabrication methods and applications of microstructured gallium based liquid metal alloys," *Smart Mater. Struct.*, vol. 25, no. 9, 2016.

27. G. Bo, L. Ren, X. Xu, Y. Du, and S. Dou, "Recent progress on liquid metals and their applications," *Adv. Phys. X*, vol. 3, no. 1, pp. 412–442, 2018.
28. J. G. Webster, M. Zou, Z. Hu, C. Hua, and Z. Shen, "Liquid Antennas," *Wiley Encycl. Electr. Electron. Eng.*, pp. 1–23, 2016.
29. K. N. Paracha, A. D. Butt, A. S. Alghamdi, S. A. Babale, and P. J. Soh, "Liquid metal antennas: Materials, fabrication and applications," *Sensors (Switzerland)*, vol. 20, no. 177, pp. 1–26, 2020.
30. E. Motovilova and S. Y. Huang, "A review on reconfigurable liquid dielectric antennas," *Materials (Basel).*, vol. 13, no. 8, pp. 1–28, 2020.
31. M. D. Dickey, "Emerging Applications of Liquid Metals Featuring Surface Oxides," *ACS Appl. Mater. Interfaces*, vol. 6, pp. 18369–18379, 2014.
32. D. Kim *et al.*, "On-demand frequency tunability of fluidic antenna implemented with gallium-based liquid metal alloy," *Eur. Phys. J. Appl. Phys.*, vol. 78, p. 11101, 2017.
33. J. Zhu and H. Cheng, "Recent development of flexible and stretchable antennas for bio-integrated electronics," *Sensors (Switzerland)*, vol. 18, no. 12, pp. 1–22, 2018.
34. M. Cosker, L. Lizzi, F. Ferrero, R. Staraj, and J. Ribero, "Realization of 3-D Flexible Antennas Using Liquid Metal and Additive Printing Technologies," *IEEE Antennas Wirel. Propag. Lett.*, vol. 16, pp. 971–974, 2017.
35. M. Zandvakili, M. M. Honari, P. Mousavi, and D. Sameoto, "Gecko-Gaskets for Multilayer, Complex, and Stretchable Liquid Metal Microwave Circuits and Antennas," *Adv. Mater. Technol.*, vol. 2, no. 11, pp. 1–5, 2017.
36. D. Morales, N. A. Stoute, Z. Yu, D. E. Aspnes, and M. D. Dickey, "Liquid gallium and the eutectic gallium indium (EGaIn) alloy: Dielectric functions from 1.24 to 3.1 eV by electrochemical reduction of surface oxides," *Appl. Phys. Lett.*, vol. 109, no. 9, pp. 1–5, 2016.
37. T. Liu, P. Sen, C. C. J. Kim, and A. C. A. Measurements, "Characterization of Nontoxic Liquid-Metal Alloy Galinstan for Applications in Microdevices," *J. Microelectromechanical Syst.*, vol. 21, no. 2, pp. 443–450, 2012.
38. M. R. Moorefiled, R. C. Gough, A. M. Morishita, J. H. Dang, A. T. Ohta, and W. A. Shiroma, "Frequency-tunable patch antenna with liquid-metal-actuated loading slot," *Electron. Lett.*, vol. 52, no. 7, pp. 498–500, 2016.
39. D. Kim, J. H. Yoo, and J. Lee, "Liquid metal-based reconfigurable and stretchable photolithography," *J. Micromech*, vol. 26, pp. 1–9, 2016.
40. J. . Dang, R. . Gough, A. . Morishita, A. . Ohta, and W. A. Shiroma, "Liquid-metal frequency-reconfigurable slot antenna using air-bubble actuation," *Electron. Lett.*, vol. 51, no. 21, pp. 1630–1632, 2015.
41. L. Song and Y. Rahmat-Samii, "Reconfigurable Patch Antenna with Liquid Metal Tuning Slots and 3D Printed Microfiuidics," *IEEE Antennas Propag. Soc. Int. Symp. Usn. Natl. Radio Sci. Meet. APSURSI 2018 - Proc.*, pp. 289–290, 2018.
42. A. P. Saghati, J. S. Batra, J. Kameoka, and K. Entesari, "A Microfluidically Reconfigurable Dual-Band Slot Antenna With a Frequency Coverage Ratio of 3:1," *IEEE Antennas Wirel. Propag. Lett.*, vol. 15, pp. 122–125, 2016.
43. A. Dey, R. Guldiken, and G. Mumcu, "Microfluidically reconfigured wideband frequency-tunable liquid-metal monopole antenna," *IEEE Trans. Antennas Propag.*, vol. 64, no. 6, pp. 2572–2576, 2016.
44. S. Singh *et al.*, "A Pattern and Polarization Reconfigurable Liquid Metal Helical Antenna," *IEEE Int. Symp. Antennas Propag. Usn. Natl. Radio Sci. Meet.*, pp. 857–858, 2018.
45. M. R. Moorefield, A. T. Ohta, and W. A. Shiroma, "A polarization-reconfigurable antipodal dipole antenna using liquid metal," *Asia-Pacific Microw. Conf. Proceedings, APMC*, pp. 1250–1252, 2018.

46. G. B. Zhang, R. C. Gough, M. R. Moorefield, K. J. Cho, A. T. Ohta, and W. A. Shiroma, "A liquid-metal polarization-pattern-reconfigurable dipole antenna," *IEEE Antennas Wirel. Propag. Lett.*, vol. 17, no. 1, pp. 50–53, 2018.
47. R. C. Gough, R. C. Ordonez, M. R. Moorefield, K. J. Cho, W. A. Shiroma, and A. T. Ohta, "Reconfigurable liquid-metal antenna with integrated surface-tension actuation," *2016 IEEE 11th Annu. Int. Conf. Nano/Micro Eng. Mol. Syst. NEMS 2016*, pp. 66–69, 2016.
48. K. J. Sarabia, S. S. Yamada, M. R. Moorefield, A. W. Combs, A. T. Ohta, and W. A. Shiroma, "Frequency-Reconfigurable Dipole Antenna Using Liquid-Metal Pixels," *Hindawi Int. J. Antennas Propag.*, vol. 2018, pp. 1–6, 2018.
49. P. Zheng, B. Zhang, J. Duan, W. Wang, and Y. Tian, "Simulation Study of Cylindrical Helical Antenna based on Liquid Metal," *Proc. 2018 IEEE 3rd Adv. Inf. Technol. Electron. Autom. Control Conf. IAEAC 2018*, pp. 1244–1247, 2018.
50. M. Shirazi, T. Li, and X. Gong, "Effects of PIN diode switches on the performance of reconfigurable slot-ring antenna," *2015 IEEE 16th Annu. Wirel. Microw. Technol. Conf. WAMICON 2015*, pp. 1–3, 2015.
51. C. W. Jung, Y. J. Kim, Y. E. Kim, and F. De Flaviis, "Macro-micro frequency tuning antenna for reconfigurable wireless communication systems," *Electron. Lett.*, vol. 43, no. 4, pp. 1–2, 2007.
52. M. S. Anwar and A. Bangert, "3D Printed Microfluidics-Based Reconfigurable Antenna," *IEEE MTT-S Int. Microw. Work. Ser. Adv. Mater. Process. RF THz Appl.*, pp. 1–3, 2017.
53. A. Vorobyov, C. Henemann, and P. Dallemagne, "Liquid Metal based antenna for wearable electronic," *2016 10th Eur. Conf. Antennas Propagation, EuCAP 2016*, pp. 1–3, 2016.
54. A. P. Saghati, S. B. Kordmahale, A. P. Saghati, J. Kameoka, and K. Entesari, "Reconfigurable Quarter-Mode SIW Antenna Employing a Fluidically Switchable Via," *IEEE Int. Symp. Antennas Propag.*, pp. 845–846, 2016.
55. J. M. Floc'h and I. Ben Trad, "Design of mechanically reconfigurable meander antenna using the galinstan liquid metal," *Loughbrgh. Antennas Propag. Conf. (LAPC 2017)*, pp. 1–4, 2017.
56. Z. Chen, H. Wong, J. Xiang, and J. Kelly, "Polarization Reconfigurable Antenna with Liquid Metal," *2018 IEEE Int. Conf. Comput. Electromagn.*, pp. 1–3, 2018.
57. M. Champion, D. Jackson, B. Cumby, and E. Belovich, "Polarization Reconfigurable Antennas Using a Liquid Metal Switching Mechanism," *IEEE Int. Symp. Antennas Propag. Usn. Natl. Radio Sci. Meet.*, pp. 415–416, 2017.
58. A. H. Naqvi and S. Lim, "Design of Polarization Reconfigurable Antenna using Liquid Metal," *Int. Symp. Antennas Propag.*, pp. 1–2, 2018.
59. W. Su, R. Bahr, S. A. Nauroze, and M. M. Tentzeris, "3D printed reconfigurable helical antenna based on microfluidics and liquid metal alloy," *2016 IEEE Antennas Propag. Soc. Int. Symp. APSURSI 2016 - Proc.*, pp. 469–470, 2016.
60. E. Erdil, K. Topalli, N. S. Esmaeilzad, O. Zorlu, H. Kulah, and O. Aydin Civi, "Reconfigurable nested ring-split ring transmitarray unit cell employing the element rotation method by microfluidics," *IEEE Trans. Antennas Propag.*, vol. 63, no. 3, pp. 1163–1167, 2015.
61. W. Su, S. A. Nauroze, B. Ryan, and M. M. Tentzeris, "Novel 3D printed liquid-metal-alloy microfluidics-based zigzag and helical antennas for origami reconfigurable antenna 'trees,'" *IEEE MTT-S Int. Microw. Symp. Dig.*, pp. 1579–1582, 2017.
62. C. Borda-Fortuny, K. F. Tong, A. Al-Armaghany, and K. K. Wong, "A low-cost fluids switch for frequency-reconfigurable vivaldi antenna," *IEEE Antennas Wirel. Propag. Lett.*, vol. 16, pp. 3151–3154, 2017.
63. M. Konca and P. A. Warr, "A frequency-reconfigurable antenna architecture using dielectric fluids," *IEEE*

 doi:10.20944/preprints202012.0232.v1

Trans. Antennas Propag., vol. 63, no. 12, pp. 5280–5286, 2015.

64. H. Tang and J. Chen, "Microfluidically frequency-reconfigurable microstrip patch antenna and array," *IEEE Access*, vol. 5, pp. 20470–20476, 2017.
65. Z. Chen and H. Wong, "Liquid dielectric resonator antenna with circular polarization reconfigurability," *IEEE Trans. Antennas Propag.*, vol. 66, no. 1, pp. 444–449, 2018.
66. Z. Chen and H. Wong, "Wideband glass and liquid cylindrical dielectric resonator antenna for pattern reconfigurable design," *IEEE Trans. Antennas Propag.*, vol. 65, no. 5, pp. 2157–2164, 2017.